
Masters Theses

Student Theses and Dissertations

Summer 2005

Effect of engine operating conditions on the size and morphology of diesel particulate emissions

Adam Neer

Follow this and additional works at: https://scholarsmine.mst.edu/masters_theses



Part of the [Mechanical Engineering Commons](#)

Department:

Recommended Citation

Neer, Adam, "Effect of engine operating conditions on the size and morphology of diesel particulate emissions" (2005). *Masters Theses*. 3732.

https://scholarsmine.mst.edu/masters_theses/3732

This thesis is brought to you by Scholars' Mine, a service of the Missouri S&T Library and Learning Resources. This work is protected by U. S. Copyright Law. Unauthorized use including reproduction for redistribution requires the permission of the copyright holder. For more information, please contact scholarsmine@mst.edu.

EFFECT OF ENGINE OPERATING CONDITIONS ON THE SIZE AND
MORPHOLOGY OF DIESEL PARTICULATE EMISSIONS

by

ADAM NEER

A THESIS

Presented to the Faculty of the Graduate School of the

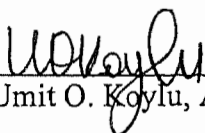
UNIVERSITY OF MISSOURI-ROLLA

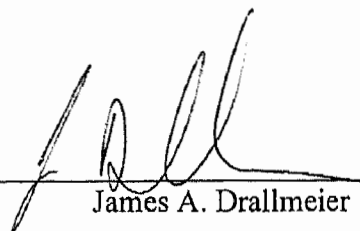
In Partial Fulfillment of the Requirements for the Degree


MASTER OF SCIENCE IN MECHANICAL ENGINEERING

2005

Approved by


Umit O. Koylu, Advisor


James A. Drallmeier


Philip D. Whitefield

ABSTRACT

The size, morphology and volume fraction of sub-micron particulate matter emitted from a compression ignition (diesel) engine was investigated using thermophoretic sampling experiments followed by direct visual characterizations under transmission electron microscopy. Specifically, measurements were conducted at the exhaust of a 6059T John Deere, 5.9 L, 6 cylinder, turbocharged, direct injection diesel engine. The particles observed were composed of nearly spherical primary particles (spherules) that formed aggregates of various sizes and shapes. The size distributions of spherules and aggregates were separately measured to obtain the available surface area, which is crucial for estimating the environmental and health impact of particles. Aggregate fractal dimensions and prefactors were also quantified. Different engine speeds and relative loads were considered to determine the effects of typical engine operating conditions on the particulate properties. The present mean spherule diameters were in the range of 20-35 nm while the mean aggregate diameters were in the range of 160 to 350 nm. 98% of the measured aggregates were smaller than a gyration diameter of 1 μm ; indicating that the current regulations based on PM(2.5) may be insufficient. Fractal dimensions and prefactors were in the range of 1.77 ± 0.14 and 1.8 ± 0.5 , respectively, characteristics of the cluster-cluster aggregation mechanism. These fractal properties are consistent with the numerous past studies in various laboratory flames and a recent study in another diesel engine. Soot volume fractions were also estimated based upon thermophoretic sampling experiments developed from laboratory flames. These measurements implemented for the first time in a diesel engine yielded soot volume fractions on the order of 0.001 to 0.01 ppm.

ACKNOWLEDGMENTS

Foremost, I would like to thank my advisor, Dr. Koylu for his motivation and the knowledge he has imparted to me during my undergraduate and graduate studies at Rolla. I would also like to thank Dr. Drallmeier for making his engine facilities available for this research, Mr. Hess for his time and assistance in running the engine, and Dr. Miller for his assistance and training with the transmission electron microscope.

A special thanks goes to the NASA-UMR Center of Excellence for Particulate Emissions Reduction Program under the leadership of Dr. Whitefield for partially sponsoring this research. I am also thankful to the department for supporting me during my studies with a teaching assistantship

And finally, I would like to thank my family for all the support they have given me throughout my academic career.

TABLE OF CONTENTS

	Page
ABSTRACT	ii
ACKNOWLEDGMENTS	ii
LIST OF ILLUSTRATIONS.....	vii
LIST OF TABLES.....	ix
 SECTION	
1. INTRODUCTION	1
2. LITERATURE REVIEW	4
2.1. INTRODUCTION	4
2.2. PAST STUDIES	4
2.3. THESIS OBJECTIVES	6
3. EXPERIMENTAL METHODS.....	7
3.1. INTRODUCTION	7
3.2. ENGINE AND ENGINE CONTROL.....	7
3.3. THERMOPHORETIC SAMPLING EQUIPMENT	8
3.4. TEM AND IMAGE PROCESSING.....	10
3.5. CALIBRATIONS	11
3.5.1. Sampling Time Calibration	11
3.5.2. TEM Magnification Calibration.....	12
3.6. TEST CONDITIONS AND PROCEDURES.....	13
4. RESULTS	15
4.1. INTRODUCTION	15

4.2. TEM OBSERVATIONS	15
4.3. SPHERULE DIAMETERS	23
4.4. AGGREGATE MORPHOLOGIES	30
4.5. AGGREGATE SIZES	35
4.6. SOOT VOLUME FRACTIONS	44
5. DISCUSSION	48
5.1. SPHERULE DIAMETERS	48
5.2. AGGREGATE SIZES.....	49
6. CONCLUSIONS AND RECOMMENDATIONS	51
6.1. CONCLUSIONS	51
6.2. RECOMMENDATIONS.....	53
APPENDIX EXPERIMENTAL UNCERTAINTIES.....	54
BIBLIOGRAPHY	57
VITA	59

LIST OF ILLUSTRATIONS

Figure	Page
3.1. John Deere 6059T diesel engine.....	8
3.2. Thermophoretic sampling set up	9
3.3. Calibration of image scale as a function of TEM magnification.....	12
4.1. TEM images taken at 13,600 magnification for two speeds at various loads	16
4.2. High magnification TEM images of two engine conditions.....	18
4.3. TEM images of particulates from various engine conditions.....	20
4.4. Production of individual spherules for three loads at 900 RPM.....	21
4.5. Production of individual spherules for three loads at 1800 RPM.....	22
4.6. Spherule size distribution for all conditions	24
4.7. Mean spherule diameter as a function of engine load	25
4.8. Mean spherule diameter as a function of overall equivalence ratio	27
4.9. Mean spherule diameter as a function of engine exhaust temperature.....	28
4.10. Mean spherule diameter as a function of engine speed	29
4.11. Number of spherules per aggregate as a function of aggregate maximum length normalized by spherule diameter for all aggregates.....	32
4.12. Area equivalent diameter as a function of maximum aggregate length	34
4.13. Percentage of particles counted as a function of aggregate gyration diameter	36
4.14. Aggregate gyration diameter size distribution for all conditions	37
4.15. Aggregate gyration diameter as a function of engine load.....	38
4.16. Aggregate gyration diameter as a function of overall equivalence ratio	39
4.17. Aggregate gyration diameter as a function of exhaust temperature	40

4.18. Aggregate gyration diameter as a function of engine speed.....	42
4.19. Area equivalent diameter as a function of engine load	43
4.20. Soot volume fraction as a function of equivalence ratio	47

LIST OF TABLES

Table	Page
3.1. Engine test conditions.....	13
4.1. Comparison of reported fractal dimensions of diesel particulates	33
6.1. Summary of particulate measurements.....	52

1. INTRODUCTION

Internal combustion engines are major sources of airborne particulates as up to 70% of the total emission inventories in urban areas are found to be related to transportation vehicles (Kittelson, 1998). The emission of these sub-micron particulates has serious health and environmental implications. Current emission standards are mainly designed for the measurement of particulate mass and therefore sizes less than 2.5 μm (PM_{2.5}) are not considered because the smaller particles contribute negligibly to the total mass. However, there is an immediate need to shift the emphasis in these regulations from mass basis to size basis because of the importance of surface area. Size and morphology is directly related the particulate transport properties, which control pulmonary deposition in the human respiratory system and residence time/chemical participation in the atmosphere. This is associated with the fact that, for a fixed mass, the particle diameter is proportional to the available surface area, which is the most essential parameter for interactions of particles with the surroundings.

Inhalation of nano-sized particles can result in severe pulmonary inflammation, increased risk of lung disease and other respiratory associated illnesses. In addition, for a given mass, smaller particles have been shown to cause more damage when compared to larger particles of identical chemistry (Warheit, 2004). Furthermore, these particles can act as carriers for other substances such as unburnt hydrocarbons, a suspected mutagen, and pollen. Particles in the atmosphere are considered a major contributor to global weather forcing. Due to the small sizes of engine produced particulates, the atmospheric residence time is larger than that of larger particles allowing them to participate in atmospheric chemistry. Also, emission of these particles to the atmosphere decreases

visibility. In addition to the health and environmental aspects, soot formation is undesirable from an engineering stand point. Soot formed in diesel engines can contribute to reduced engine life by entrainment into engine lubricants increasing frictional losses. Soot can also contribute to carbon deposits in spark ignition engines, potentially causing auto ignition or “knock”.

Soot is formed during fuel-rich combustion and much of the research on soot formation relies on studies of laboratory flames. The formation of soot is divided into different processes: pyrolysis, inception, surface growth and coagulation, aggregation and oxidation (Neeft et al., 1996). During the pyrolysis-inception process, gas phase molecules breakdown to form soot precursor species, most notably acetylene, which then form soot nuclei. During the surface growth process, growth is controlled by two mechanisms: chemical interaction and coagulation. The coagulation growth process is when individual soot nuclei combine to form a larger particle while growth through chemical interaction is thought to be sustained by the soot precursors responsible for particle inception. These processes are responsible for the formation of primary particles. Primary particles interact to form the complex fractal like structures known as aggregates that are subject to oxidation from high combustion temperatures. Aggregates observed under transmission electron microscopes show have a wide variety of shapes and sizes and consist of tens to hundreds of primary particles of nearly uniform diameters.

Particulate sizes from diesel engines have commonly been reported in the past by using mobility aerosol sizers. These commercially available instruments measure a “mobility diameter”, which does not properly characterize the combustion-generated particulates in the form of fractal aggregates of small spherical primary particles

(spherules). An overall dimension couples the spherule and aggregate sizes and consequently misleads the actual total surface area of particulates (Van Gulijk et al., 2003). Moreover, there are critical issues with respect to the aerosol dilution systems for sampling particulates from the engine exhausts. In particular, particle size distributions seem to be significantly modified by the dilution rate and pretreatment of the particles along the extensive sampling lines.

Although the actual size and morphology of soot particulates from laminar and turbulent flames are well known, there is little data for diesel engines (Lee et al., 2002; Zhu et al., 2004). Fractal dimensions that have been reported in the literature based on different techniques also appear to be broad and high (in the range of 2 to 3; Skillas et al., 1998) compared to the typical values from laboratory flames. For this purpose, quick thermophoretic sampling followed by direct electron microscope observations is utilized. This experimental technique has been well established in its ability to completely characterize the physical properties of fine particles. Thermophoretic deposition of particles relies on the temperature difference between the aerosol being sampled and the collection surface, for the present case, a TEM grid. The benefits of thermophoretic sampling over other methods is that it is a direct sampling technique requiring no pretreatment of the aerosol being sampled, and that there is minimal disruption of the aerosol flow field. This gives an accurate representation of the particles produced from the combustion environment. Collected particles can then be imaged under an electron microscope and all necessary measurements for their characterization can then be made.

2. LITERATURE REVIEW

2.1. INTRODUCTION

This section details with the published literature on diesel particulate matter as well as the different measurement techniques used. The conclusion of this section will contain the objective of this thesis.

2.2. PAST STUDIES

Much of the past work measuring soot has involved laboratory flames, with a limited amount of work done on the measurement of engine particulates. Many of the existing measurements are performed using commercial aerosol sizers such as differential mobility sizers (DMA) or scanning mobility particle sizers (SMPS). These commercial instruments require extensive dilution of the aerosol to be sampled (Kittelson, 1998), which may alter the recorded particle size. Aggregate sizes reported using these measurements are called mobility diameters, made on the assumption that engine particles are spherical in nature. However, combustion generated particles are known to be fractal in nature (Koylu et al., 1995), (Hu et al., 2003). In the work performed by Van Gulijk et al., (2004), size selected soot was measured from a light duty single cylinder diesel engine by a SMPS and low pressure impactor (LPI). Van Gulijk et al., concluded from this study that the performance of the SMPS was affected by the fractal nature of the soot and would overpredict aggregate size compared to the actual diameters as measured from a scanning electron microscope using samples collected from the LPI. Skillas et al., (1998) concluded from the study of a Yamaha diesel generator that diesel soot fractal dimensions would vary significantly with engine load and should be in the

range of 2 to 3. These measurements were based upon mobility measurements coupled with an LPI. Recently Park et al., (2004) measured diesel particulates from a medium duty John Deere diesel using both electron microscopy and mobility techniques. It was concluded from this study that mobility diameter is nearly equal to an aggregates projected area diameter, key in relating fractal dimensions as measured by mobility sizers to those by electron microscopy.

Eisner and Rosner, 1985 concluded that the dominant mechanism for soot transport and deposition was by thermophoresis rather than random particle motion, and that deposition by thermophoresis relies on particle sizes being less than the gas mean-free path, implying size biasing is possible. Thermophoresis is the process of particle drift in the thermal boundary layer in the gases near the collection surface. From this work thermophoretic sampling techniques coupled with electron microscopy have been developed for use in laboratory flames (Dobbins and Megaridis, 1987), (Koylu et al., 1995), (Hu et al., 2003). The benefits of this methodology are that it is a direct sample of the sooty exhaust gases, and that it can provide information on soot primary particle size, aggregate size, fractal properties and an estimate for soot volume fractions. Lee et al., (2002) measured soot properties of aggregates sampled from a heavy duty diesel engine for multiple engine speeds and loads using thermophoretic techniques with transmission electron microscope (TEM) analysis, the first time this sampling method was used in a diesel engine. Zhu et al., (2004) measured engine soot from various loads and speeds using techniques identical to Lee et al., (2002) for a light duty diesel engine. Both Lee et al., (2002) and Zhu et al., (2004) observed that soot properties have a dependence on engine load.

2.3. THESIS OBJECTIVES

The goal of this study is to quantify the soot size distribution and morphology at the exhaust of a diesel engine utilizing thermophoretic sampling techniques. Measurements will then be made at various engine speeds and loads to determine the effect of engine condition on mean primary particle (spherule) diameters, overall aggregate sizes and fractal dimensions and prefactors. Additionally estimates for exhaust soot volume fraction will be made in order to determine the range of volume fractions emitted from a diesel engine as well as the effect of engine load on soot volume fractions.

3. EXPERIMENTAL METHODS

3.1. INTRODUCTION

This section is to describe in detail the complete experimental set up used. This will include the specifics of the engine test cell, thermophoretic sampling device, and transmission electron microscope operation. The details of measurements will be covered along with experimental procedures and the experimental conditions considered.

3.2. ENGINE AND ENGINE CONTROL

The type of engine used was a turbocharged 6059T John Deere medium duty diesel engine, with a peak power of 123 kW at 2500 RPM and peak torque of 538 N-m at 1600 RPM. The engine displacement is 5.9 L with an inline six cylinder configuration, operating with a compression ratio of 17.8 to 1. Fuel was supplied using a rotary injection pump with mechanical governor. For the duration of the experiments the engine was fueled by a number 2 diesel fuel from a 1000 gallon tank shared by other engines, which was refilled during the course of the measurements. Fuel was supplied by the MFA Oil Company and is specified as a low sulfur diesel fuel. The fuel has a minimum cetane number of 45 with a sulfur maximum percentage weight of 0.05. Fuel flow measurements were provided using a positive displacement flow meter on a fuel cart separate from the engine. Air flow into the engine was measured using a laminar flow element. Engine exhaust temperatures were measured with thermocouples on both the manifold and exhaust pipe. The engine speed was controlled by a Westinghouse D.C. dynamometer with load controlled by the engine operator. A photograph of the engine used for sampling is included as Figure 3.1.

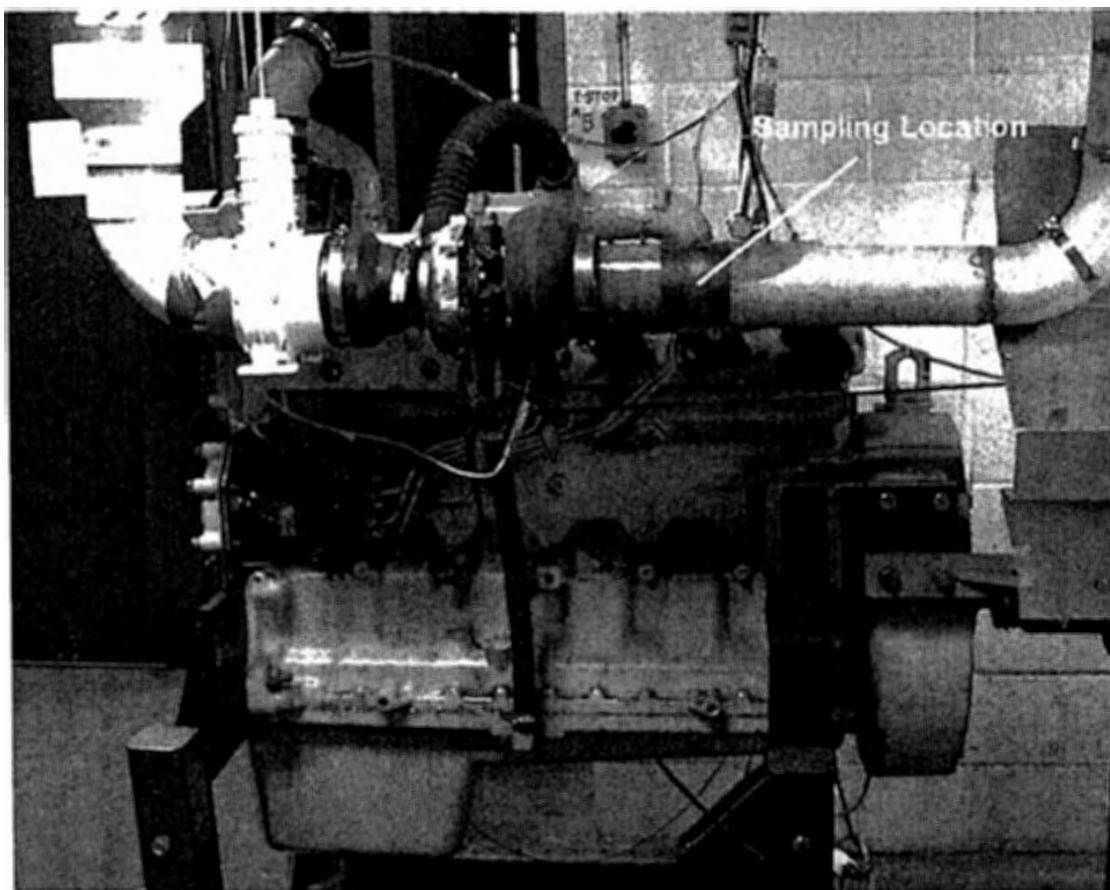


Figure 3.1. John Deere 6059T diesel engine

3.3. THERMOPHORETIC SAMPLING EQUIPMENT

For particle measurements thermophoretic sampling coupled with transmission electron microscopy was used. The techniques and sampling equipment used for this study was similar to those used by Dobbins and Megaridis (1987), Koylu and Faeth (1992) and Hu et al., (2003). The benefit of this sampling methodology is that no conditioning of the aerosol is needed and, that the rapid sampling provides a 'snap-shot' of the particulates in the aerosol with minimum intrusiveness. A sketch of the thermophoretic sampling equipment is provided in Figure 3.2.

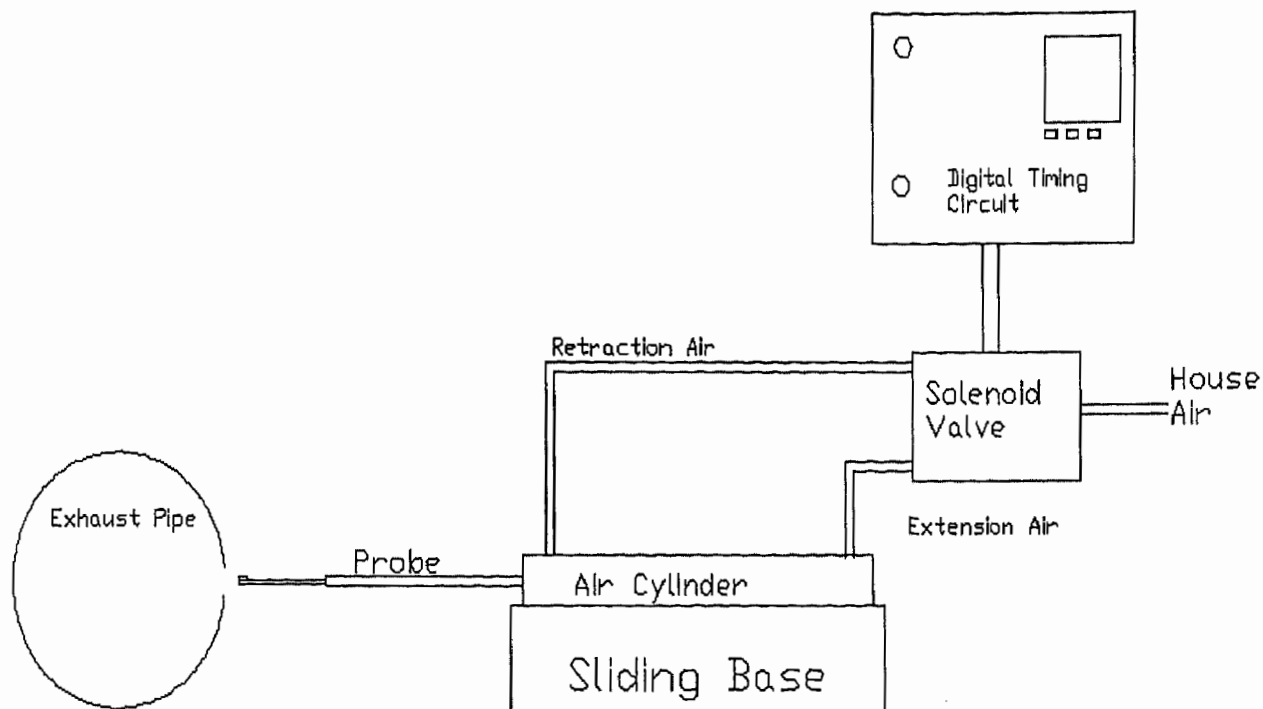


Figure 3.2. Thermophoretic sampling set up

The sampling was performed at a location after the engines turbocharger at a single location within the exhaust stream for each condition. The soot particles were collected on 3mm Copper TEM grids with a carbon film backing. Grids were special orders from the Electron Microscopy Sciences Company, (CF-H4-Spec-Cu). TEM grids were adhered to the sampling probe using a small amount of white glue placed on the probe. The grid was then positioned so that a thin annular area around the grid was the point of contact. Typically more than one contact point was needed do to the high exhaust gas velocities where sampling occurred. The material choice for the probe was a stainless steel. The probe used for the experiments was 13mm long, with a base width and thickness of 6 mm and 1 mm respectively. The area which was inserted into the exhaust

stream parallel to the flow had a length of 5 mm with a width of 2.8 mm and thickness of 0.5 mm in order to facilitate minimum disruption to the flow of exhaust gases. The base of the probe was drilled and tapped in order to fit the threaded end an air cylinder (Bimba 0074-DXP). A (Aro A212SS-12-A) four-way solenoid valve controlled the probe action by switching between two sets of ports controlling the extension and retraction of the probe. The compressed air used to run the valve was supplied by engine lab house air, which is at a pressure of 80 psi. The valve was actuated by a digital timer (Omron H5CR-B), which precisely controlled the actuation of the ports on the solenoid valve with timing precision down to 1 millisecond.

3.4. TEM AND IMAGE PROCESSING

Used TEM grids were stored in a grid storage box provided by the manufacturer until needed at TEM. A Philips EM430T transmission electron microscope was used to capture high magnification photographs of soot particles. The microscope can operate at 50 to 100 kV with magnifications ranging from 50 to 750,000 with a resolution of 0.24 nm. For the present study photographs were taken at an accelerating voltage of 100 kV with magnifications in the range of 10,300 to 88,600. Lower magnifications were used in for making aggregate measurements, while higher magnifications were used for spherule measurements. Images were usually under focused in order to provide optimum contrast between the carbon soot and the carbon film background. Because of this photography technique, Fresnel rings were present around the edges of the particles which introduce measurement errors using the image analysis software.

Due to the fact that soot concentration was nearly insensitive to grid position in the exhaust flow stream photographs were taken at various locations across the grid surface. Magnifications above 42,500 were used in making spherule diameter measurements while magnifications in the range of 10,300 to 21,200 were used in measuring aggregate sizes and soot volume fractions. Magnifications lower than 10,300 were not considered due to the inability to resolve the aggregates accurately to account for their fractal like structure. Photographs were taken using traditional methods by exposing Kodak electron microscope film (SO-163). Exposed negatives were removed from the microscope and developed using classic darkroom techniques using Kodak developer fluid and rapid fixer. In order to ensure the preservation of negatives, they were dipped into a photo-flow solution in order to sheen off all water after rinsing. Developed films were digitized by using a scanner with a transparency adapter (Epson Perfection 1200U). Images were scanned at a resolution of 600 dpi and saved as JPEG formats. During the scanning process image adjustments were made using the scanning software (Adobe Photodeluxe BE R1) in order to provide better image contrast for image analysis. Image measurements were made using image processing software (Media Cybernetics, Image-Pro Plus R1.3).

3.5. CALIBRATIONS

3.5.1. Sampling Time Calibration. Sampling time directly contributes to the exposure of the grid surface to the exhaust stream. This is critical for catching a large amount of soot aggregates for analysis, while not providing too much coverage of the grid surface. Sampling times varied from 100 ms to upwards of 700 ms. The large

variation of sampling times is due to a decrease in soot production at lower engine loads coupled with a decrease in exhaust gas temperature at the sampling location. Larger sampling times were required at lower engine loads with shorter times at high loads. Sampling time calibration was performed using the same system prior to these experiments. A linear relationship between the preset time on the timer t_p , and the actual sampling time t_s , was then obtained:

$$t_s = 0.9758t_p - 8.2111 \quad (1)$$

3.5.2. TEM Magnification Calibration. Image measurements were made in pixels, requiring a conversion ratio from pixels to nm for each magnification. A conversion factor was obtained by capturing images of 312 nm latex calibration spheres (Electron Microscopy Sciences – 80030) and then applying the same techniques used in the analysis of aggregates. Calibration ratios were calculated by dividing the pixel diameter by the actual size, calibration ratios were determined for the various magnifications considered. The resulting calibration curve is shown in Figure 3.3.

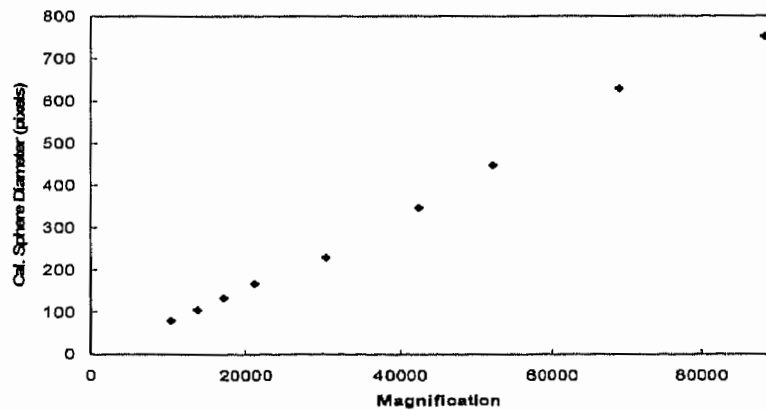


Figure 3.3. Calibration of image scale as a function of TEM magnification

3.6. TEST CONDITIONS AND PROCEDURES

The goal of these experiments was to determine how soot properties depended on engine operating conditions, specifically engine speed and load. Speed was quantified by the revolutions per minute of the engines crankshaft, known as RPM. Load was considered in terms of a relative load, a percentage of the maximum torque produced at a given speed. Engine load could range from 0 % to 100 %, with zero loads corresponding to idling conditions. For the present work loads were ranged from 10% load to 100% load, and speeds ranged from 900 RPM to 1800 RPM for a total of 15 conditions. A summary of engine operating conditions is included in Table 3.1.

Table 3.1 Engine test conditions

Speed	Load
900 RPM	10%
	50%
	100%
1000 RPM	50%
	70%
	95%
1300 RPM	50%
	70%
	95%
1700 RPM	50%
	70%
	95%
1800 RPM	10%
	50%
	100%

Prior to sampling a three-stage warm up was used to get the engine to operating temperature. The engine was motored at 800 RPM for 5 minutes, and then fired at a load of 100 lb-ft at 1000 RPM for another 5 minutes, and then 200 lb-ft at 1000 RPM for a final 20 minutes. After warming up the engine was held at a sampling condition for an additional 5 to 10 minutes to allow the engine exhaust temperatures to reach steady-state. During this time the grid was placed on the probe to allow the glue to dry. After the engine reached steady state the probe was placed on the air cylinder and the probe was rapidly inserted into the exhaust stream. Immediately after sampling the TEM grid was carefully removed from the probe and placed in the protective grid box.

4. RESULTS

4.1. INTRODUCTION

Soot spherule diameters, d_p , aggregate projected area, A_a , and maximum aggregate length, L , were measured directly from digitized TEM images. Properties of principal interest are: spherule diameter, aggregate diameter of gyration, d_g , aggregate projected area diameter, d_a , fractal pre-factor, k_f , fractal dimension, D_f , and soot volume fraction, f_v . These values will be reported as mean values for each condition, with experimental uncertainties provided in the appendix. Discussion of spherule and aggregate sizes are included in a later section.

4.2. TEM OBSERVATIONS

Figure 4.1 are typical TEM photographs of three loading conditions at an engine speed of 1000 RPM. As the engine load increased, a higher concentration of soot aggregates were deposited onto the grid surface when compared to the lower loading conditions, a trend observed in a recent study by Lee et al., (2002). This phenomenon was observed for the range of engine speeds considered and was strategic in choosing sampling times. It should be noted that the sampling time was increased at lower engine loads, but soot coverage was always 15% or less of an image area in order to prevent any artificial overlapping of aggregates on the sampling grids.

Aggregates collected from the engine were polydisperse in both size and shape, composed of nearly spherical monodisperse primary particles (spherules). This observation has been made by previous studies of diesel engines (Wentzel et al., 2003, Braun et al., 2003, Skillas et al., 1998) as well as experiments involving laboratory

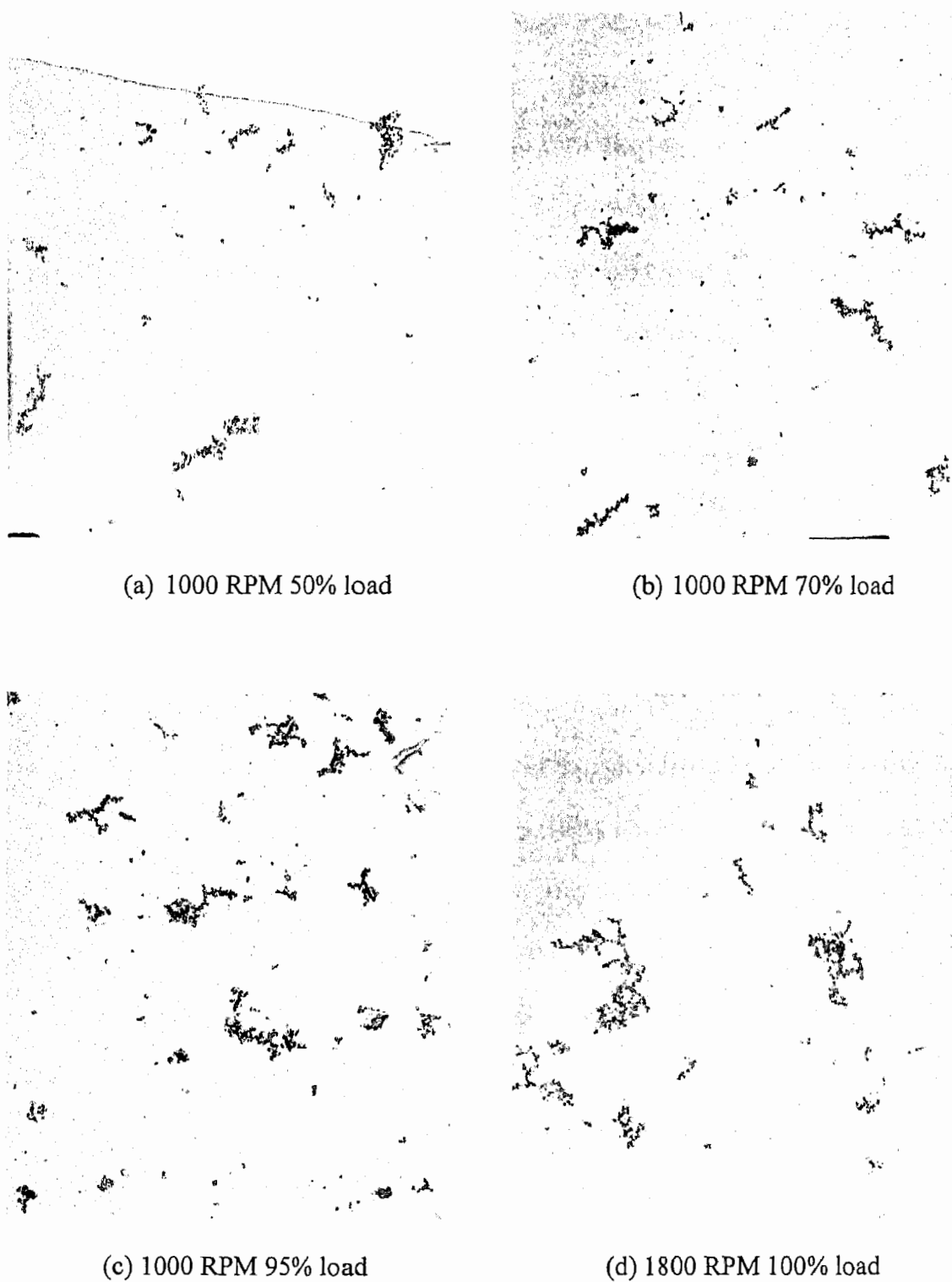
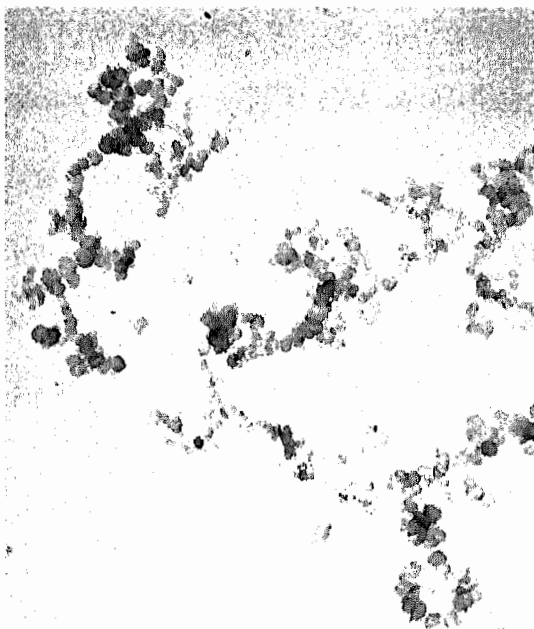


Figure 4.1. TEM images taken at 13,600 magnification for two speeds at various loads

flames (Hu et al., 2003). In addition to the aggregate concentration, aggregate sizes appeared to increase with increasing load, a trend which will be discussed later on.

The TEM photographs in Figure 4.2 are high magnification images in which the internal structure of diesel aggregates can be observed for two different engine conditions. For the higher loading condition the aggregates were larger and the spherules that compose the aggregates were well-defined. The aggregate sampled from the lower loading condition was more compact in shape with an internal structure that was indistinct in comparison; however, aggregates with well defined structure can also be produced at lower loads. In two independent studies by Lee et al.,(2002) and Zhu et al., (2004), the soot structure at higher engine loads was characterized as distinct graphitic crystalline structures, while aggregates at lower loads were described as being amorphous for two different diesel engines. From these experiments, the crystalline structure of soot was analyzed by Raman scattering and attributed to high temperatures. The classification of amorphous soot structures relied solely on TEM observations, from which it was conjectured that amorphous soot contained a high concentration of soluble organic compounds. For the present study, a graphitic structure was not discernable in aggregates collected at high engine loading conditions, while compact amorphous aggregates appeared to be produced at lower loads.

Over-all, aggregate structures are fractal like in nature and have been characterized by a fractal dimension representing the complex morphology. Skillas et al., (1998) reported that aggregates form either ballistically (monomer-cluster) or by a diffusion-limited (cluster-cluster) mechanism, with distinct fractal dimensions for each.



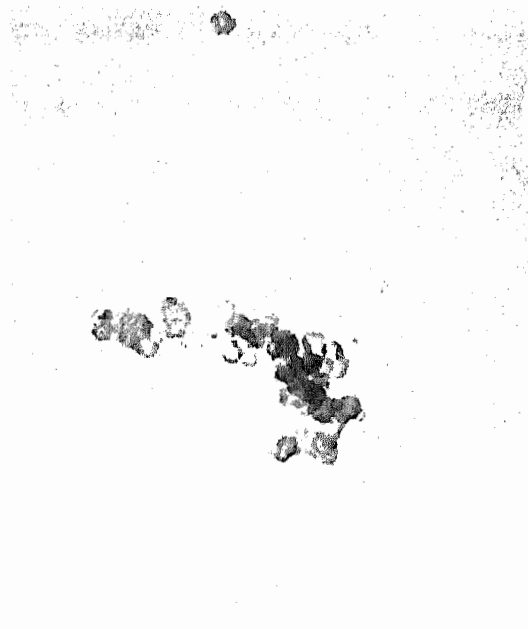
(a) 900 RPM, 100% load, 100 kV,
52,100 magnification



(b) 900 RPM, 100% load, 200 kV,
160,000 magnification



(c) 900 RPM, 100% load, 200 kV,
340,000 magnification

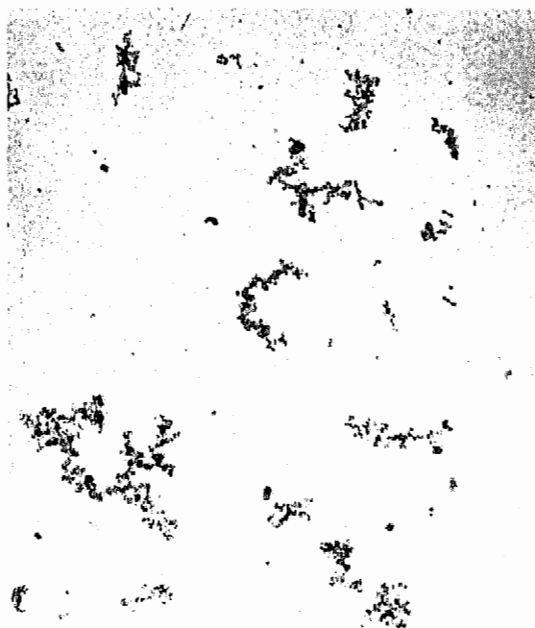


(d) 1800 RPM, 10% load, 100 kV,
88,600 magnification

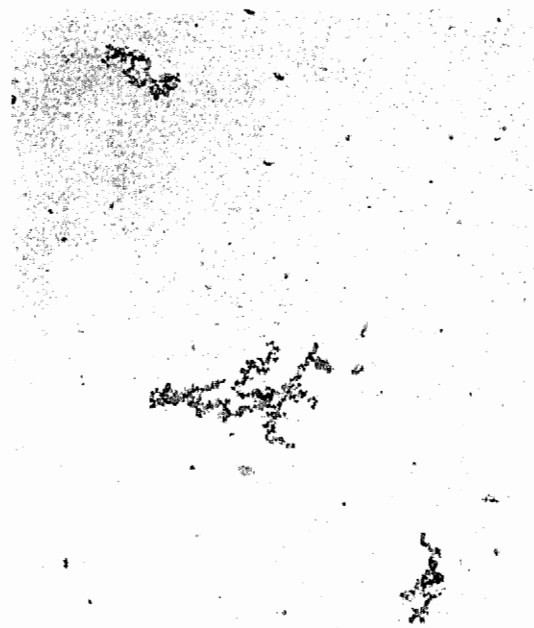
Figure 4.2. High magnification TEM images of two engine conditions

As a consequence of this, aggregates formed from the two mechanisms should look distinctive during TEM analysis and the fractal dimensions should vary significantly with load. For the present study, images from various conditions are presented in Figure 4.3. Upon observation, aggregates from the cluster-cluster regime seem to be dominant. Aggregates formed from the cluster-cluster agglomeration method are a composite formed from other aggregates identifiable by the variation of spherule size within the larger formation. This might be attributed to the formation of spherules in different localized combustion regions. These cluster-cluster aggregates tend to be larger in size and a more complex shape than monomer-cluster aggregates. Monomer-cluster aggregates are identified by their more compact shape and uniform spherule size distribution within the aggregate. Monomer-cluster aggregates were emitted, but in insignificant numbers when compared to the amount of cluster-cluster aggregates measured. The measured values for the fractal dimension were associated with cluster-cluster aggregates, indicating that this formation mechanism was dominant for the range of engine conditions.

Aggregates composed of tens to hundreds of spherules were produced at all engine loads and speeds. In addition to these larger aggregates, unaggregated spherules were also emitted from the engine. This observation is important in that these smallest particles pose a serious health risk and are unregulated by current legislation by the US EPA. Figures 4.4 and 4.5 are TEM images for the two different engine speed conditions. As the load increased the presence of these spherules in the exhaust stream increased, that is, higher engine loads produced more of these ultra-fine particles. Park et al., (2004) observed small spherule clusters being emitted from a John Deere diesel engine at



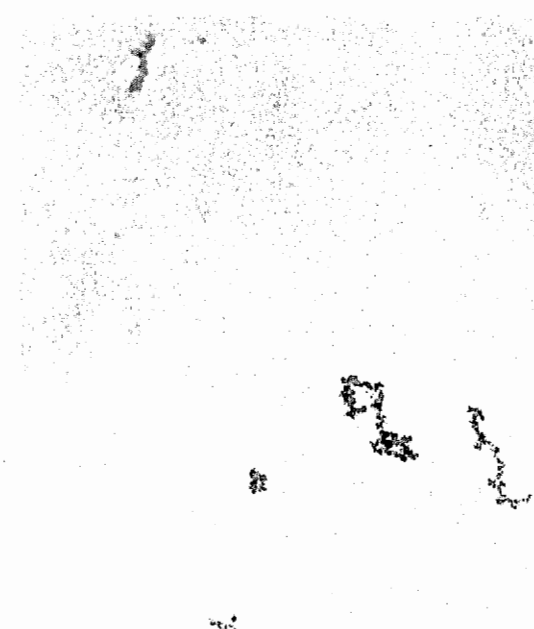
(a) 900 RPM, 100% load,
17,100 magnification



(b) 1000 RPM, 50% load,
17,100 magnification

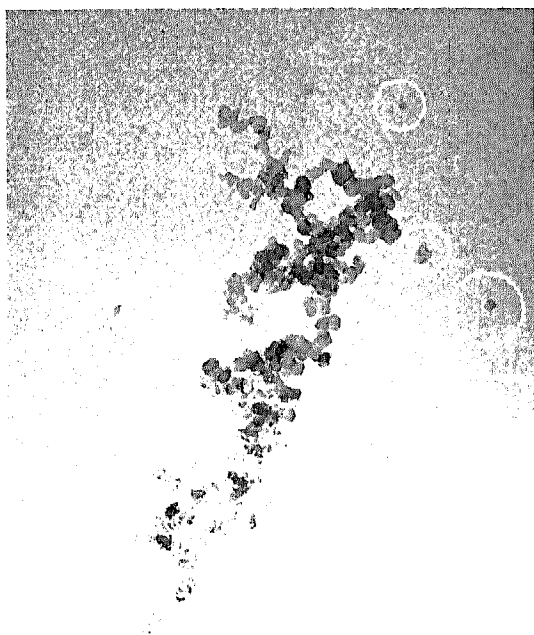


(c) 1300 RPM, 70% load,
13,600 magnification

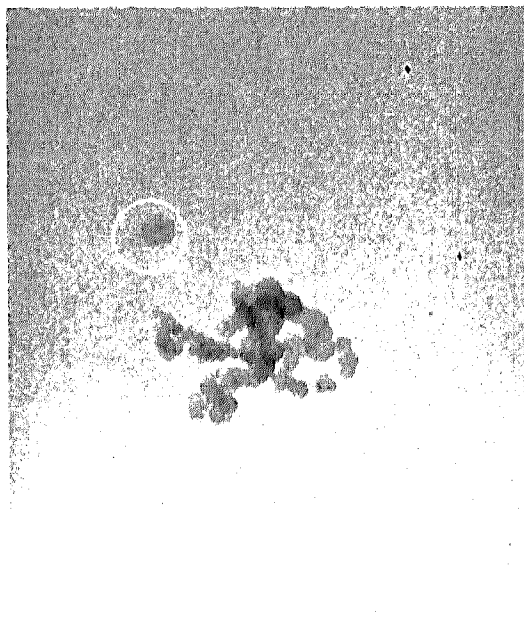


(d) 1800 RPM, 10% load,
17,100 magnification

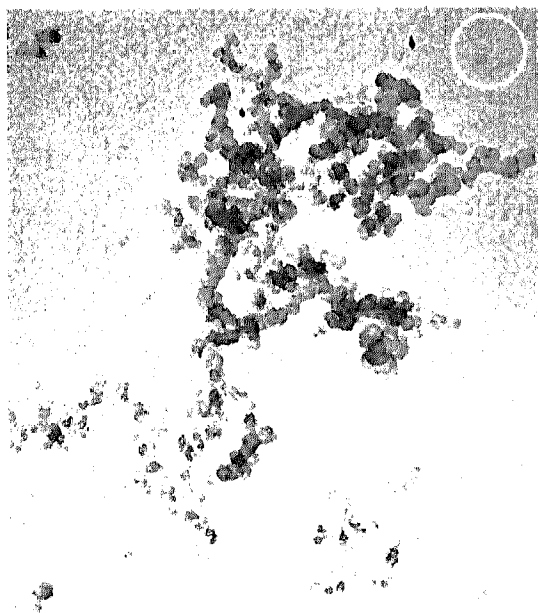
Figure 4.3. TEM images of particulates from various engine conditions



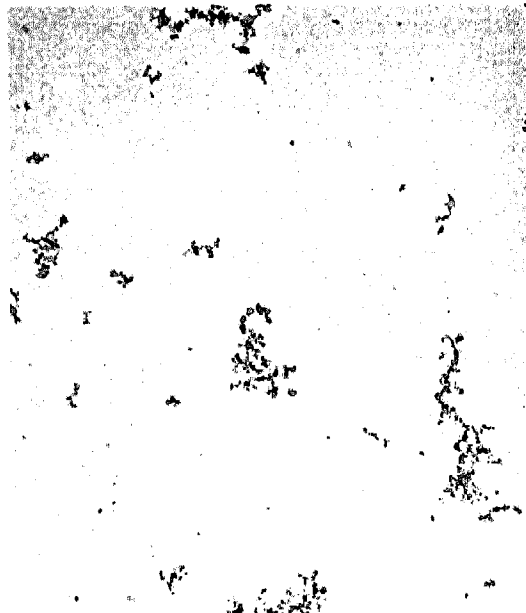
(a) 900 RPM, 10% load,
42,500 magnification



(b) 900 RPM, 50% load,
88,600 magnification

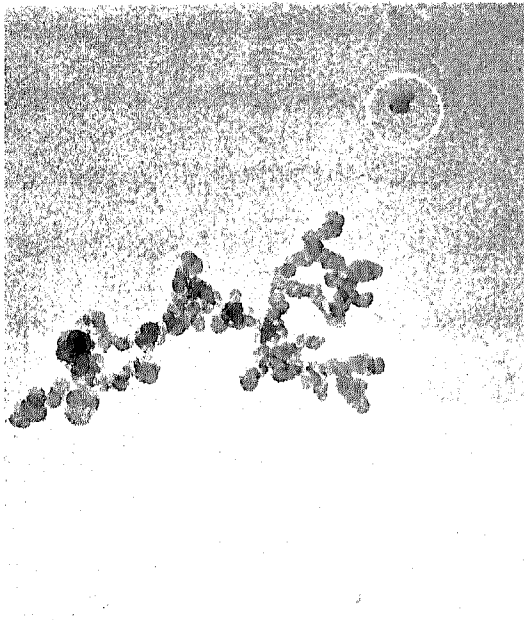


(c) 900 RPM, 100% load,
52,100 magnification

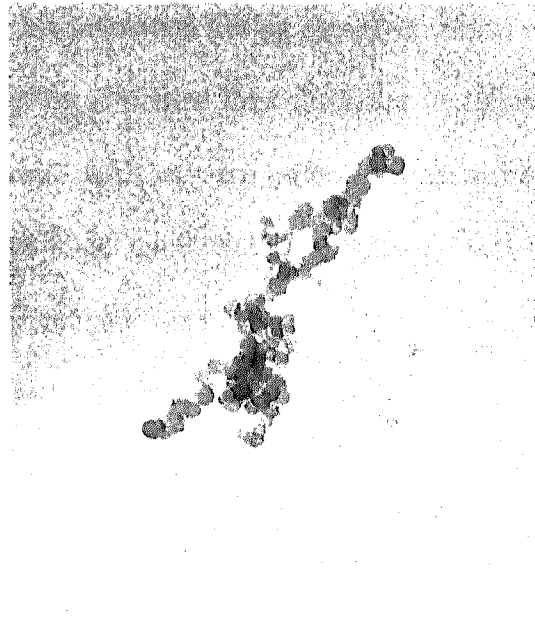


(d) 900 RPM, 100% load,
13,600 magnification

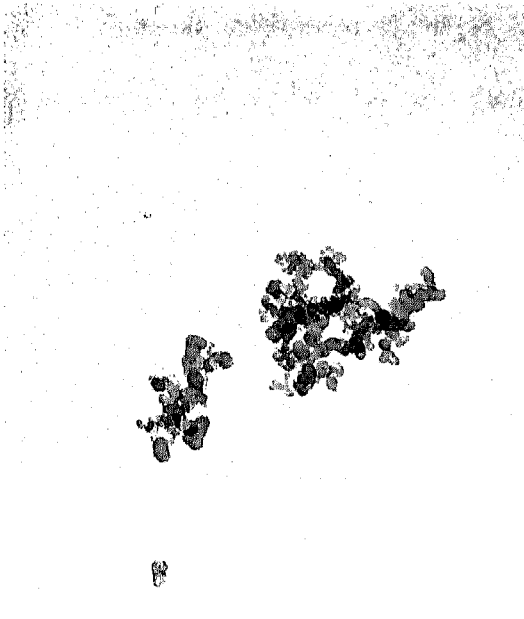
Figure 4.4. Production of individual spherules for three loads at 900 RPM



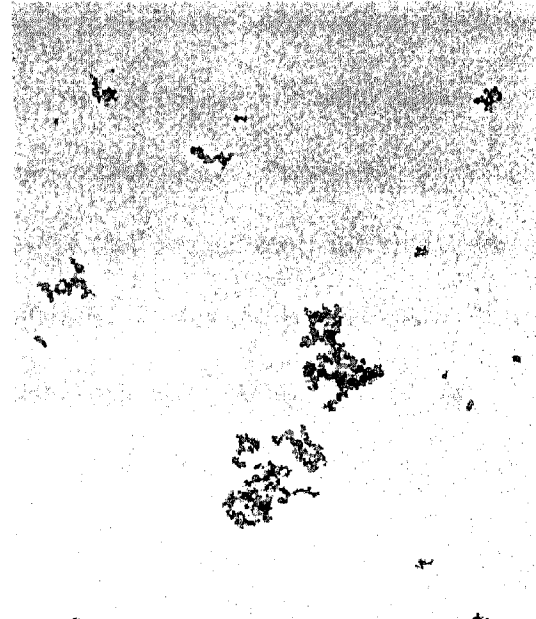
(a) 1800 RPM, 10% load,
69,000 magnification



(b) 1800 RPM, 50% load,
88,600 magnification



(c) 1800 RPM, 100% load,
69,000 magnification



(d) 1800 RPM, 100% load,
13,600 magnification

Figure 4.5. Production of individual spherules for three loads at 1800 RPM

moderate load, but attributed them to particle fragmentation during sampling. Shi et al., (2004) also observed these individual particles but attributed their formation to dilution techniques. For the present work these individual particles were collected from a probe inserted parallel to the flow so aggregate break-up upon impact is unlikely and no dilution was used in collecting samples. Also, samples were collected after the engines turbocharger. It would not seem feasible that the mechanical components of the turbocharger would fragment aggregates because of the difference in size scale when compared to the turbocharger. More research needs to be conducted on these individual particles.

4.3. SPHERULE DIAMETERS

Spherule diameters, d_p , were individually measured at each engine conditions from multiple aggregates. Of principal interest were the effects of engine relative load, overall equivalence ratio, exhaust temperature and engine speed. Previously Koylu et al. (1992) and Park et al. (2004) showed that flame and engine soot spherule sizes are normally distributed by sampling of about 200 particles. For the present study sample sizes were typically 20-50 particles with standard deviations being 20% of the mean. Experimental distributions for each engine condition, along with a fitted normal distribution from all measurements are shown in Figure 4.6.

Mean spherule diameter trends with respect to engine load are illustrated in Figure 4.7. As the engine load increased, spherule diameters tended to increase, with sizes ranging from 20 to 35 nm. Lee et al., (2002) reported a size range of 29 to 35 nm for a heavy diesel engine while experiments by Braun et al., (2004) reported a mean diameter

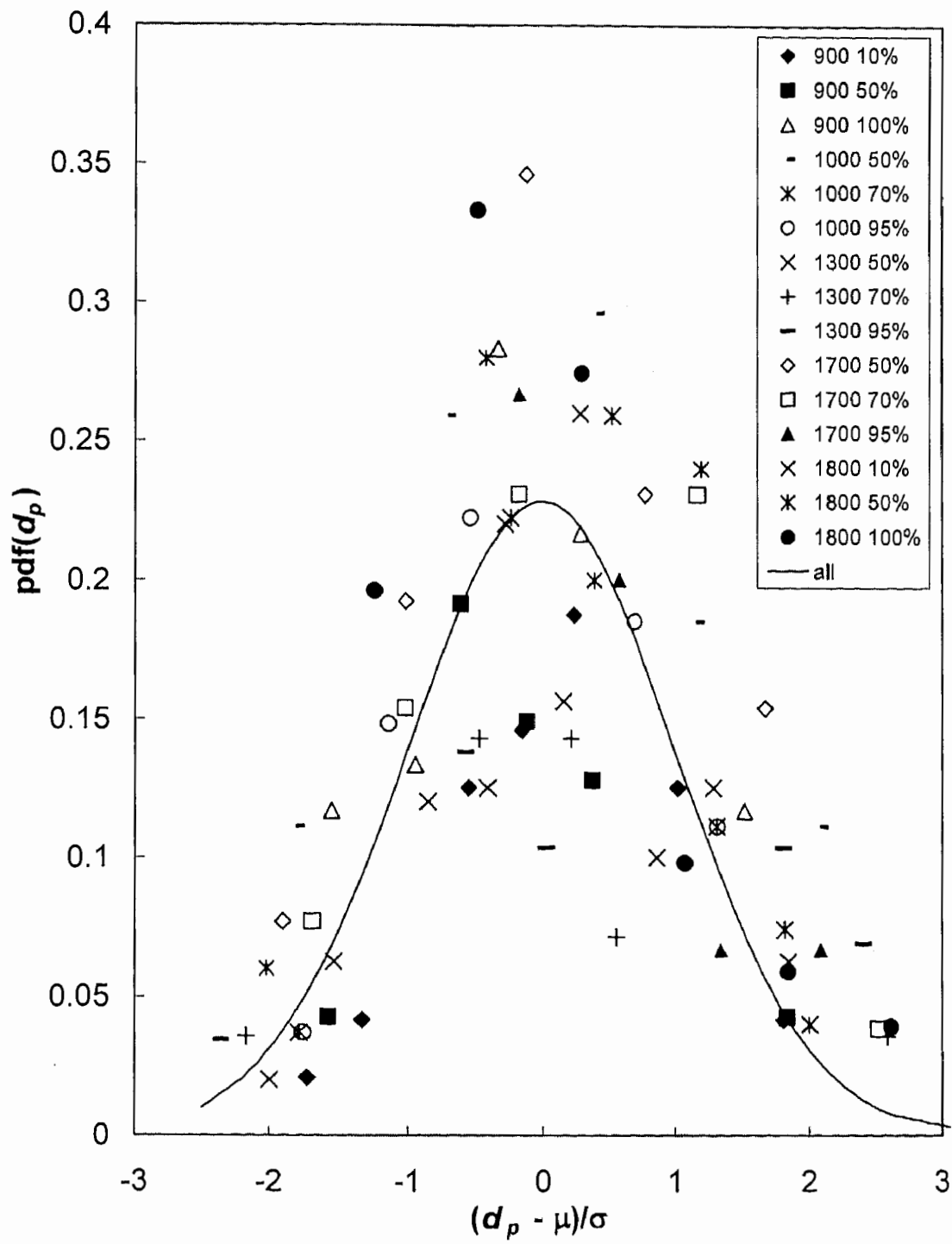


Figure 4.6. Spherule size distribution for all conditions

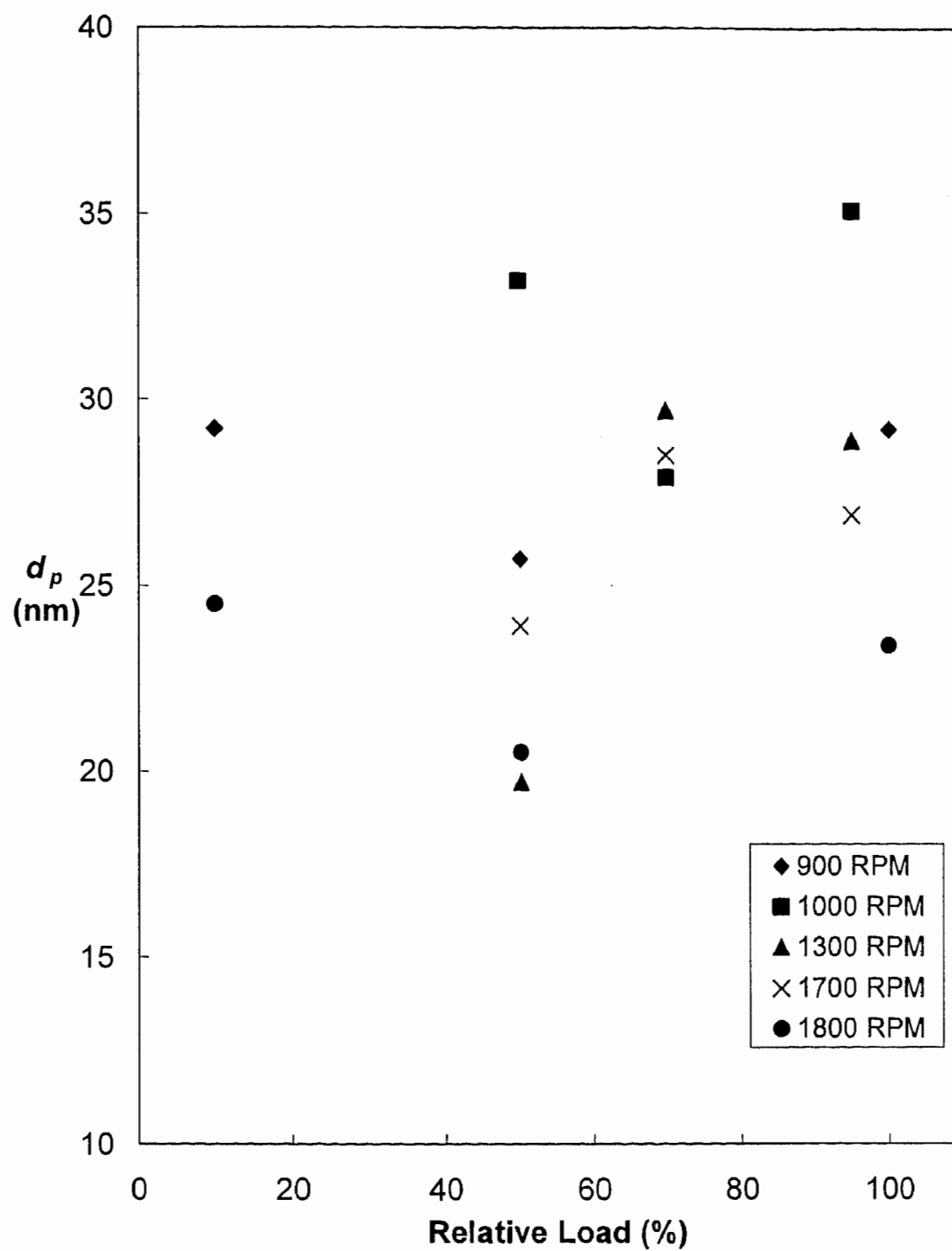


Figure 4.7. Mean spherule diameter as a function of engine load

of 15 nm for a two-stroke diesel measured at a single operating condition. For diesel engines, load is controlled by the amount of fuel injected into the cylinder. An engine operating condition can be characterized by an overall equivalence ratio, Φ . The trend for spherule diameter as a function of overall equivalence ratio is illustrated in Figure 4.8. As the equivalence ratio increased, measured spherule diameter size clearly increased as well. Engine exhaust temperatures are dependent upon engine load, which is in turn a function of the overall equivalence ratio. Spherule diameter trends as a function of exhaust temperature are shown in Figure 4.9 along with measurements made by Zhu et al., (2004). An interesting result is that these two independent studies report nearly the same size range but with two different trends with respect to exhaust temperatures. Arguments for the increase of spherule diameter with respect to increases in exhaust temperature are similar to those related to engine load, or equivalence ratio, since exhaust temperature is proportional to these two variables. Zhu et al., (2004) accounts for their trend by higher combustion temperatures with increasing load, presuming that temperature is the dominant factor in formation and oxidation of these particles.

The effect of engine speed on the spherule size was also considered. The observed trend for this engine was that spherule size was decreasing with increasing engine speed, as illustrated in Figure 4.10. Engine speed is related to the characteristic time for soot formation, which can contribute to soot growth and oxidation. Work done by Lee et al., (2002) involving a heavy duty diesel determined that the characteristic time had little affect in contributing to particle growth, while measurements by Zhu et al., (2004) from a light duty engine reported that residence time appeared to effect spherule diameter.

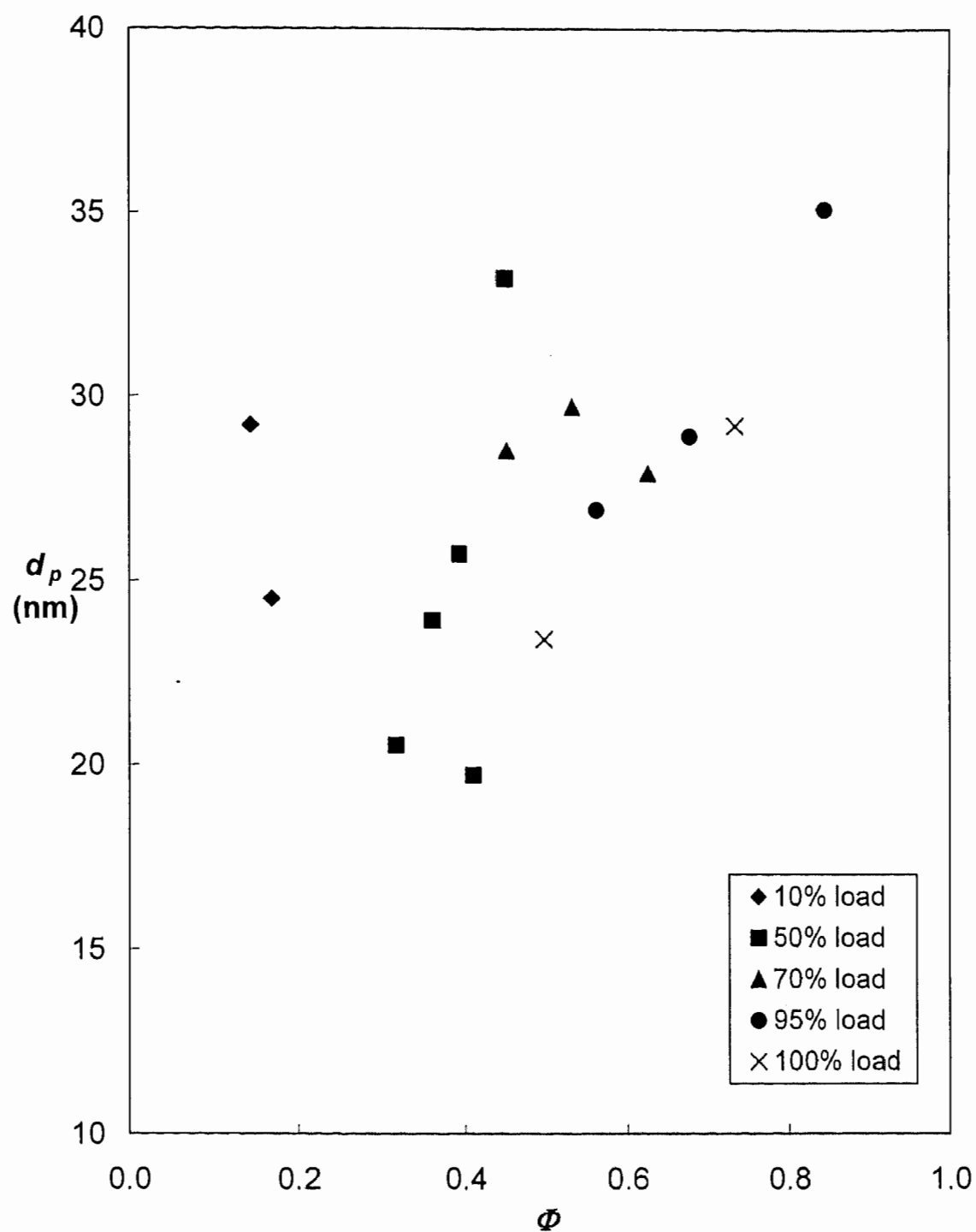


Figure 4.8. Mean spherule diameter as a function of overall equivalence ratio

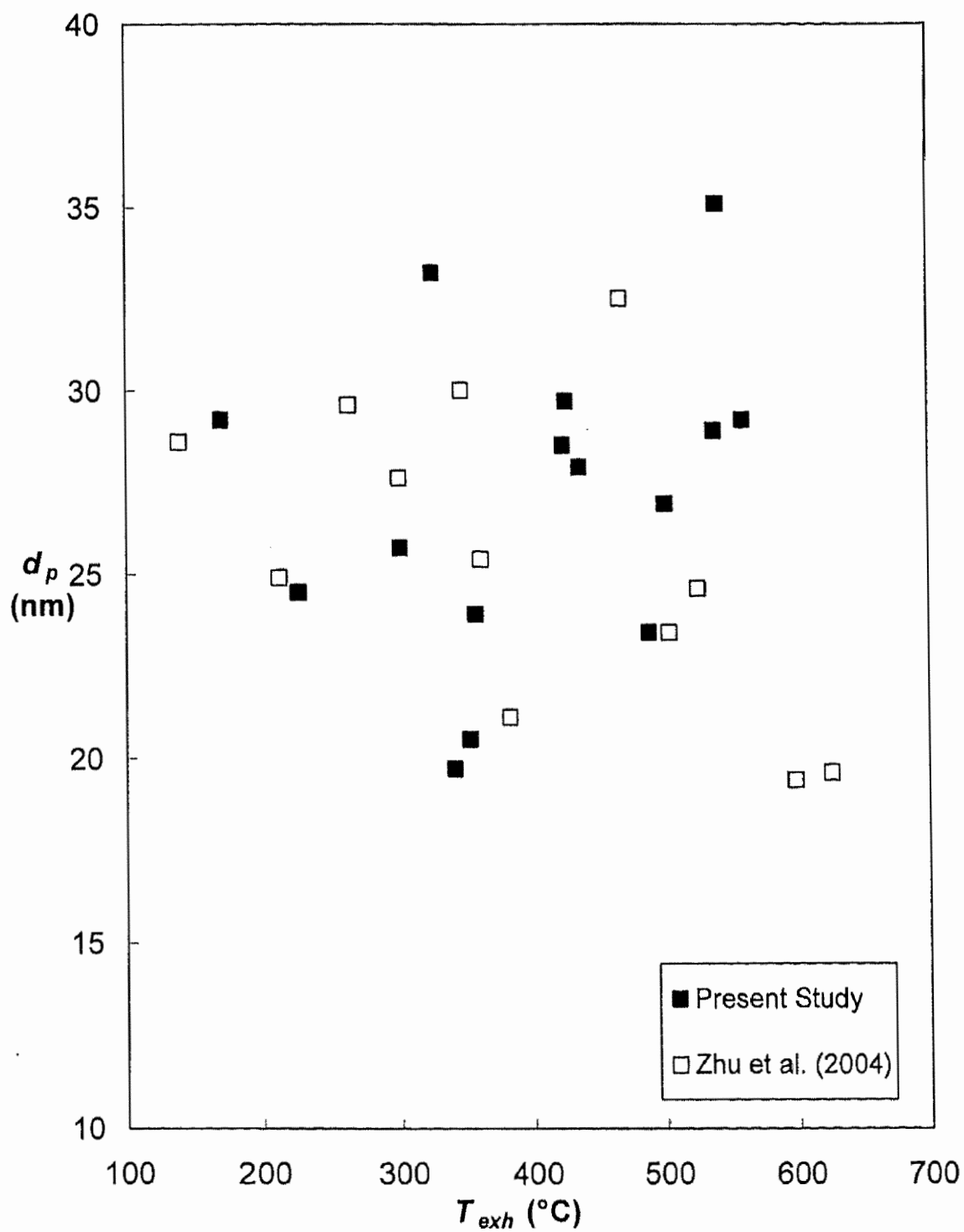


Figure 4.9. Mean spherule diameter as a function of engine exhaust temperature

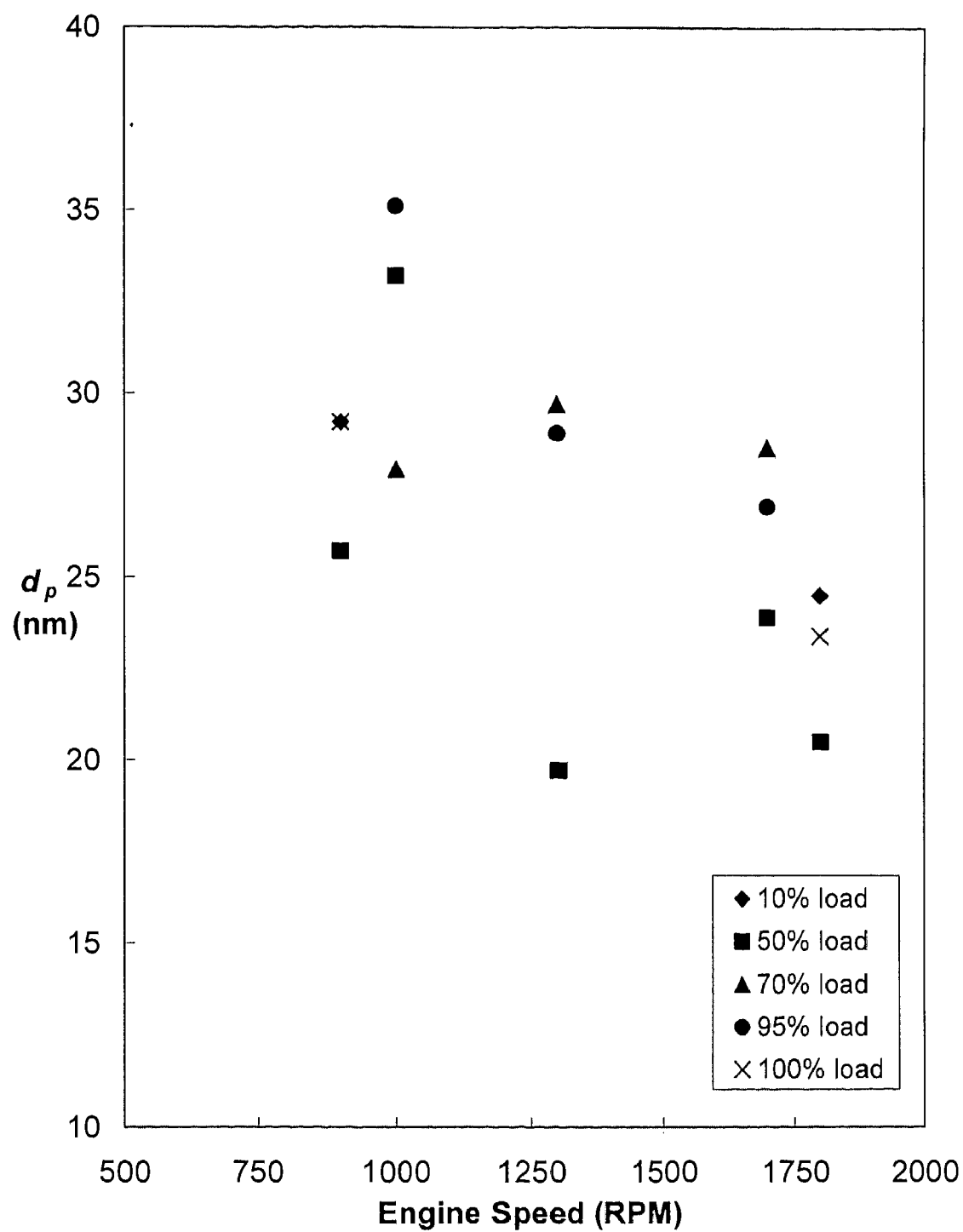


Figure 4.10. Mean spherule diameter as a function of engine speed

4.4. AGGREGATE MORPHOLOGIES

For morphological measurements of the diesel aggregates, the following statistical relationships were used following Koylu et al., (1995):

$$N = 1.15 \left(\frac{A_a}{A_p} \right)^{1.09} = k_L \left(\frac{L}{d_p} \right)^{D_f} = k_f \left(\frac{d_g}{d_p} \right)^{D_f} \quad (2)$$

In these equations, N is the number of primary particles, A_a is the projected two-dimensional aggregate area, A_p is the projected area of a primary particle, d_p is the primary particle diameter, D_f and k_f are the fractal dimension and fractal pre-factor respectively, L is the maximum length of an aggregate as measured from TEM, and k_L is a correlation constant.

Using the correlations in equation 2, fractal dimensions and fractal pre-factors were calculated by measuring aggregate projected areas and maximum aggregate length for 50 to 100 aggregates at each engine condition. Log-log plots of N versus L/d_p were made to obtain the fractal dimensions ranging from 1.65 to 1.92 for all the engine conditions considered in this study. The correlation constant, k_L , was converted to the fractal prefactor, k_f , using (Koylu et al., 1995).

$$\frac{k_f}{k_L} = \left(\frac{D_f + 2}{D_f} \right)^{\frac{D_f}{2}} \quad (3)$$

The measured fractal prefactors ranged from 1.3 to 2.4 for the present medium-duty diesel engine. Figure 4.11 illustrates all the aggregate data, yielding an average fractal dimension of 1.76 and average correlation constant of 0.95, which corresponds to an average fractal prefactor of 1.8. Both the fractal dimension and pre- factor are needed to fully characterize the soot aggregates emitted from diesel engines. There is a rather limited amount of studies involving diesel soot morphology while there has been detailed in work involving laboratory flames. The fractal dimensions measured from this diesel engine are comparative to those reported from turbulent flames by Hu et al., (2003). This provides motivation for the continued study of these flames for experimental modeling combustion and soot formation.

Of the work involving diesel morphology, most measurements are made using electron microscopy with limited attempts to characterize diesel morphology using aerosol sizers. A recent study by Park et al., (2004) used TEM measurements to develop a correlation between morphology measurements made by aerosol sizers and TEM. They claimed that aggregate mobility diameter was equivalent to aggregate projected area diameter, which is in relation to aggregate projected area. The correlation between TEM measurements and mobility diameter was then proposed as:

$$L \sim D^{\alpha}_{projected} \sim D^{\alpha}_{mobility} . \quad (5)$$

Further development of the correlation in equation 5 leads to the following equation:

$$D_{fm} / \alpha = D_{\mu} . \quad (6)$$

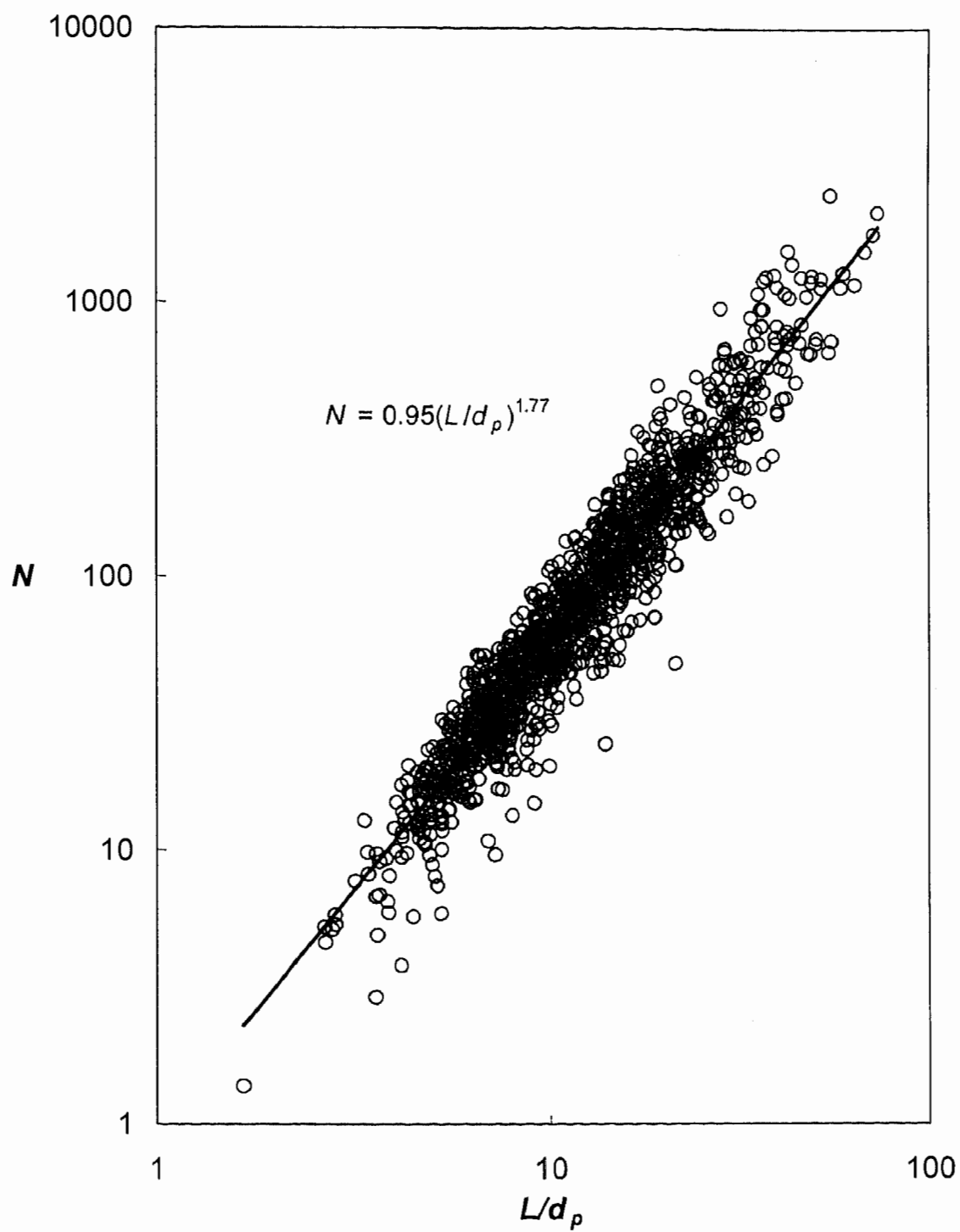


Figure 4.11. Number of spherules per aggregate as a function of aggregate maximum length normalized by spherule diameter for all aggregates

relating the fractal dimension from TEM measurements to those of mobility. It should be noted that with α greater than 1, the fractal dimension for mobility measurements will be greater than that of TEM, consistent with what has been reported in the literature (Skillas et al., 1998). Fractal properties reported by various studies are summarized in Table 4.1. The relationship of maximum length to projected area diameter in Figure 4.12 was developed with measurements from the current diesel engine, with $\alpha = 1.13$, close to the value of 1.26 by Park et al., (2004).

Table 4.1 Comparison of reported fractal dimensions of diesel particulates

Reference	Diesel Engine Type	D_f	k_f
Present study	6 cylinder John Deere engine, various loads and speeds	1.65-1.92	1.3-2.4
Zhu et al. (2004)	Light-duty engine, various loads and speeds	1.46-1.70	N/A
Lee et al. (2002)	Heavy-duty engine, single cylinder, 4 conditions	1.80-1.88	N/A
Park et al. (2004) ¹	4 cylinder John Deere engine, single operating condition	1.75	2.21
Wentzel et al. (2003) ²	Unknown engine, Single operating condition	1.70	1.9-4.0
Skillas et al. (1998) ³	Yamaha EDA 3000 engine, various loads	2.1-2.9	-

¹ Reported data was re-calculated to determine fractal prefactor.

² Only 5-7 aggregates were measured.

³ Using a mobility analyzer.

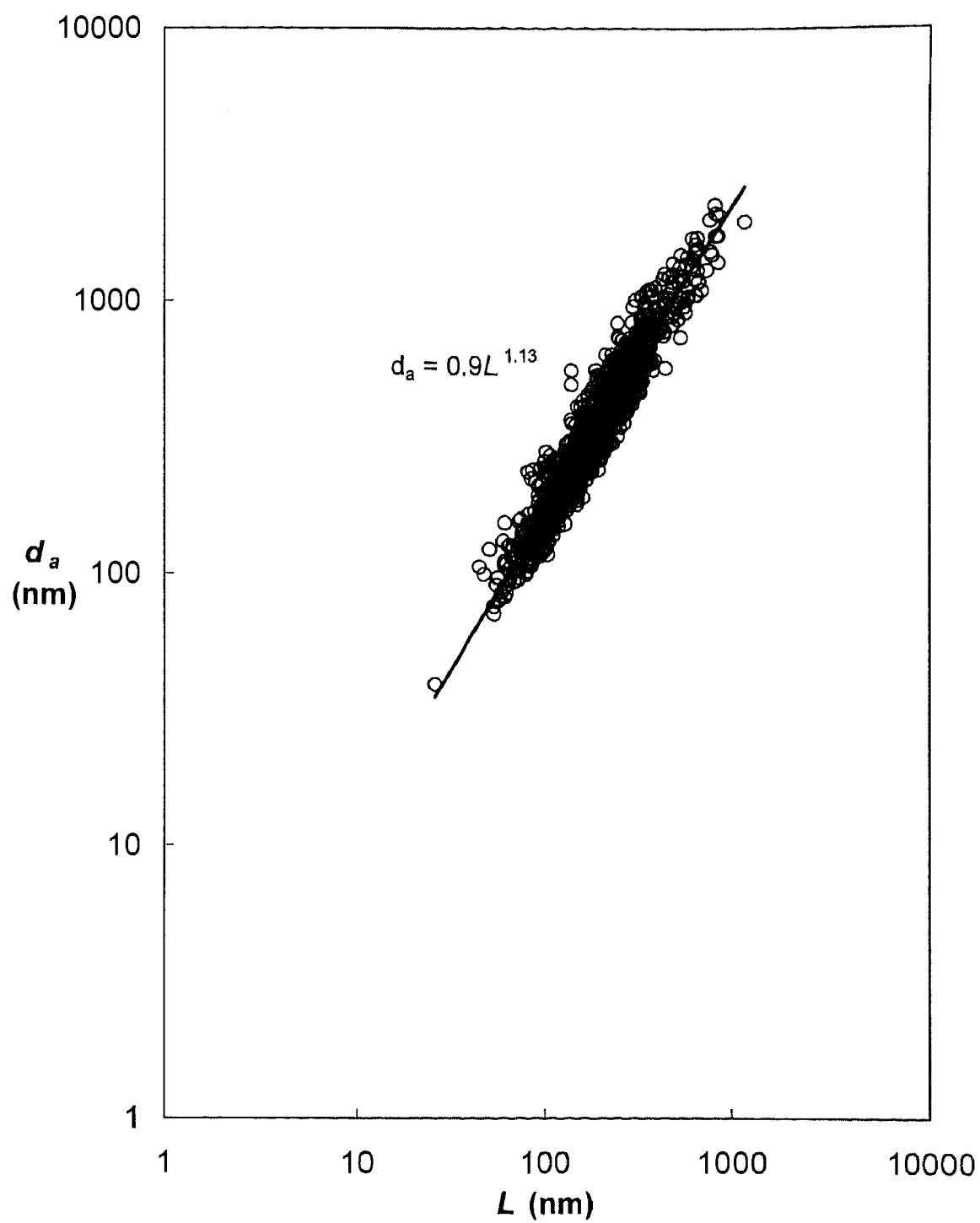


Figure 4.12. Area equivalent diameter as a function of maximum aggregate length

4.5. AGGREGATE SIZES

Aggregate sizes were measured on the basis of the gyration of diameter, d_g . After determining the fractal properties at each engine condition, the gyration diameter was obtained from the relationship in equation 2. Aggregate mean diameter of gyration ranged from 160 to 350 nm for the range of engine conditions. With over 1200 aggregates measured, the majority fell into this median range with only a few particles as large as 1 μm . This observation is illustrated graphically in Figure 4.13. Over ninety percent of the particles measured were below a diameter of gyration of 0.5 micron with roughly 98% below 1 micron.

From previous measurements by Koylu and Faeth (1992) and Harris and Maricq (2001), aggregate sizes are expected to follow lognormal distributions. For each engine condition measurements for 50 to 100 aggregates were made. The experimental distributions for all available engine conditions are shown in Figure 4.14, along with a fitted lognormal distribution generated for all measurements.

Similar to spherule size, trends for mean aggregate size were also considered for engine load, equivalence ratio, exhaust temperature and engine speed. For the current measurements, mean aggregate sizes somewhat increased with increased load, as seen in Figure 4.15. As engine equivalence ratio increased, aggregate diameters increased as well, a trend illustrated in Figure 4.16. The trend for aggregate size as a function of exhaust temperature is also shown in Figure 4.17, along with aggregate diameters measured by Zhu et al., (2004). Oxidation was not noticed at higher manifold temperatures as reported by Zhu et al., (2004), leading to larger aggregate sizes with increased temperature. The aggregates formed at higher engine temperatures were

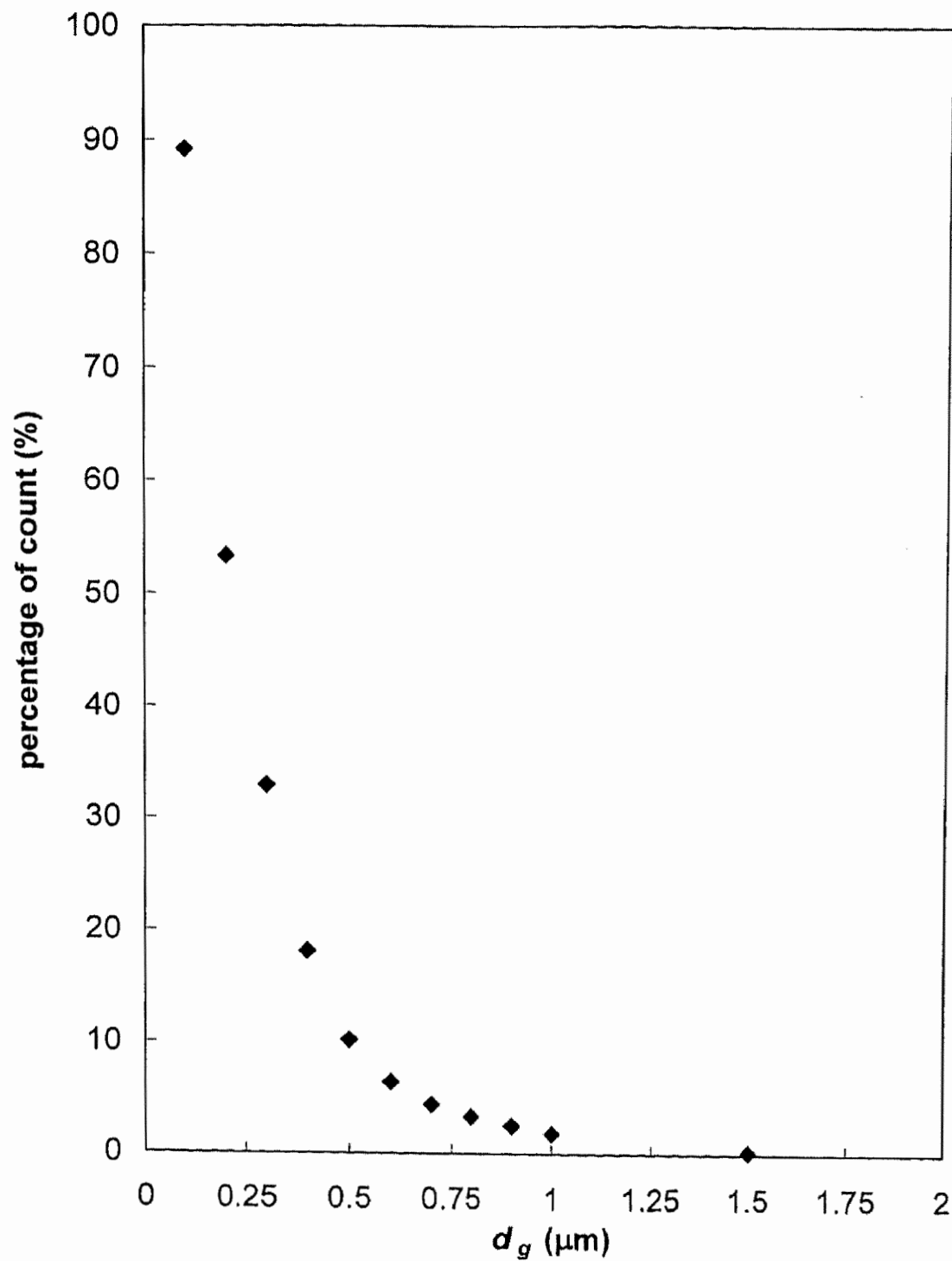


Figure 4.13. Percentage of particles counted as a function of aggregate gyration diameter

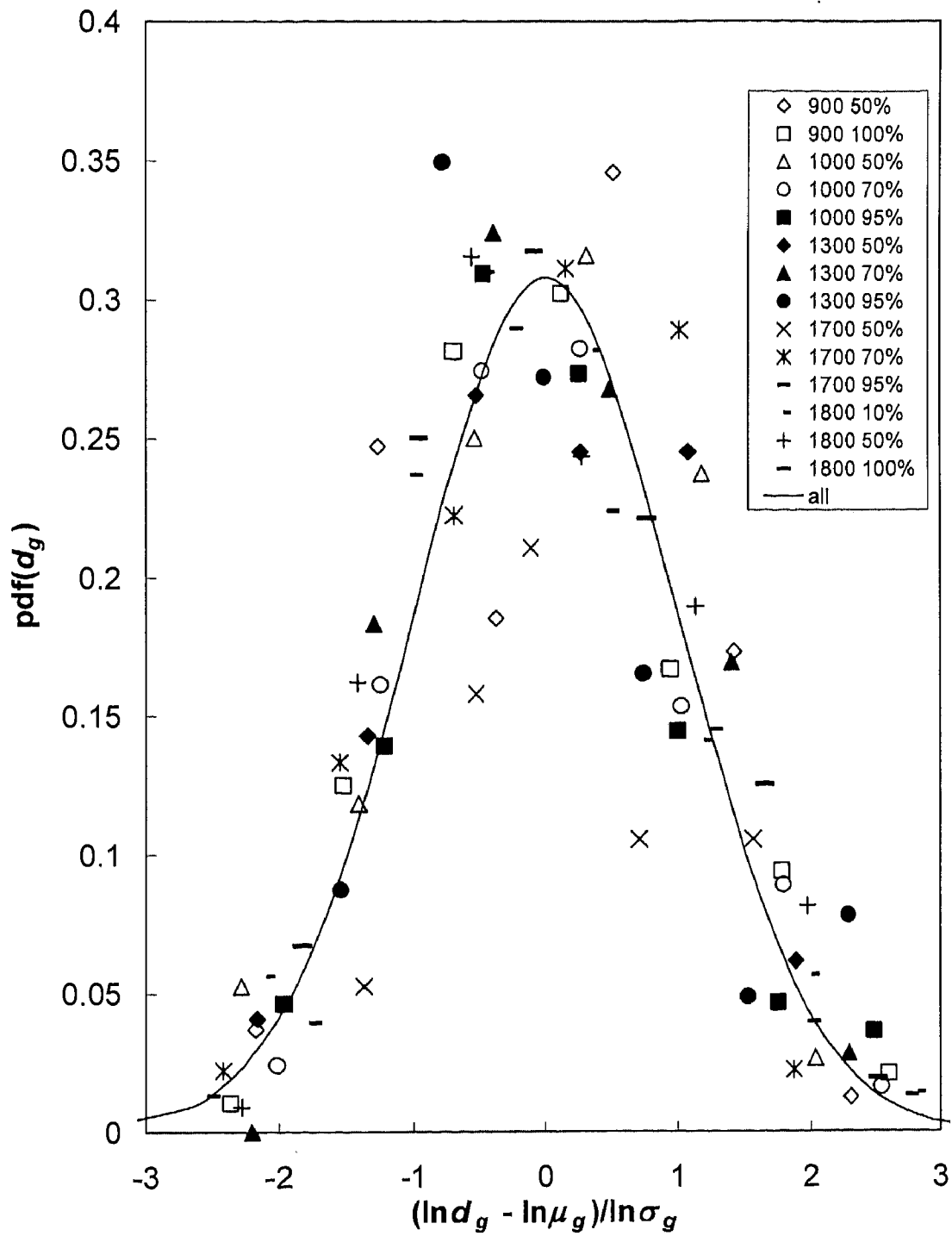


Figure 4.14. Aggregate gyration diameter size distribution for all conditions

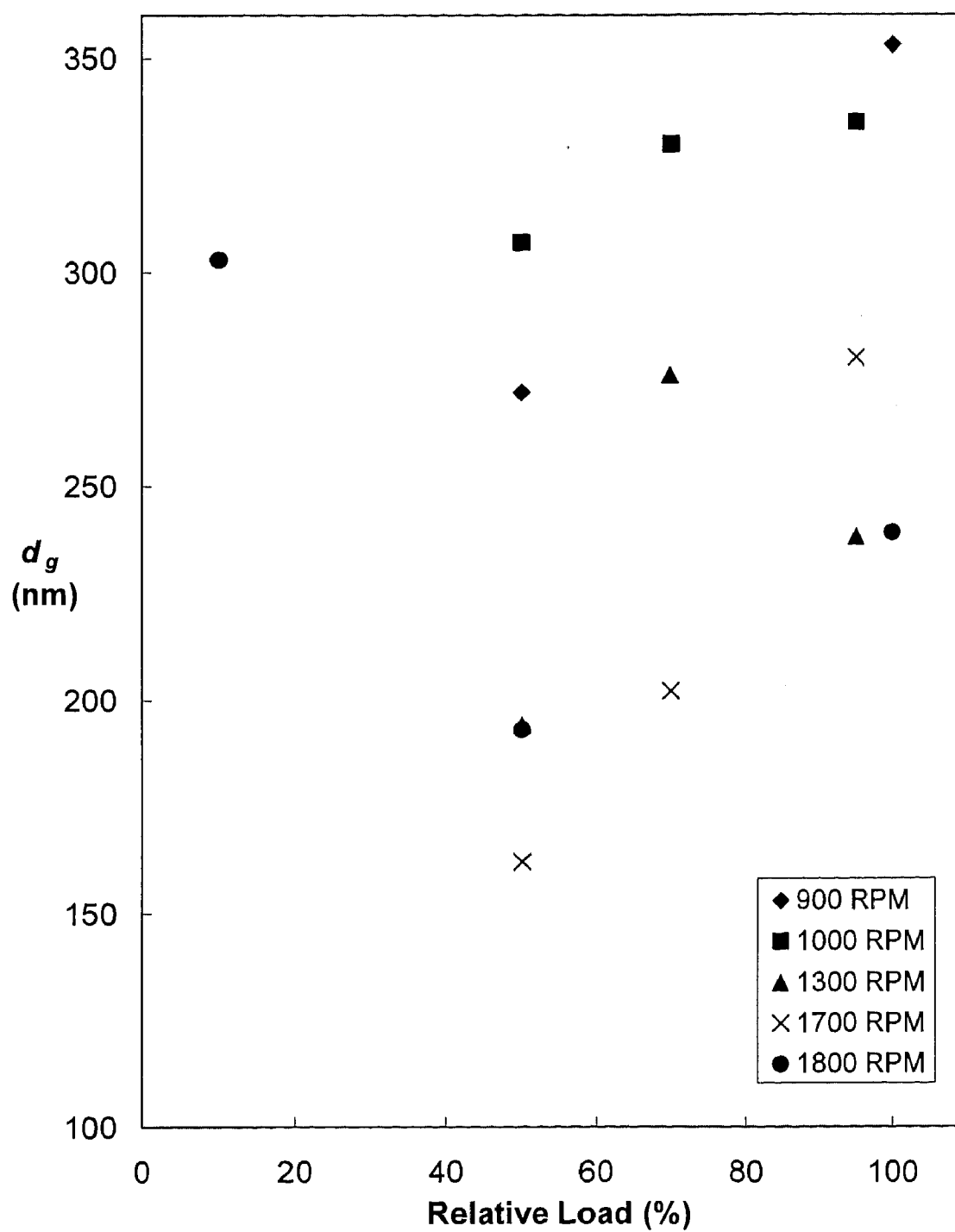


Figure 4.15. Aggregate gyration diameter as a function of engine load

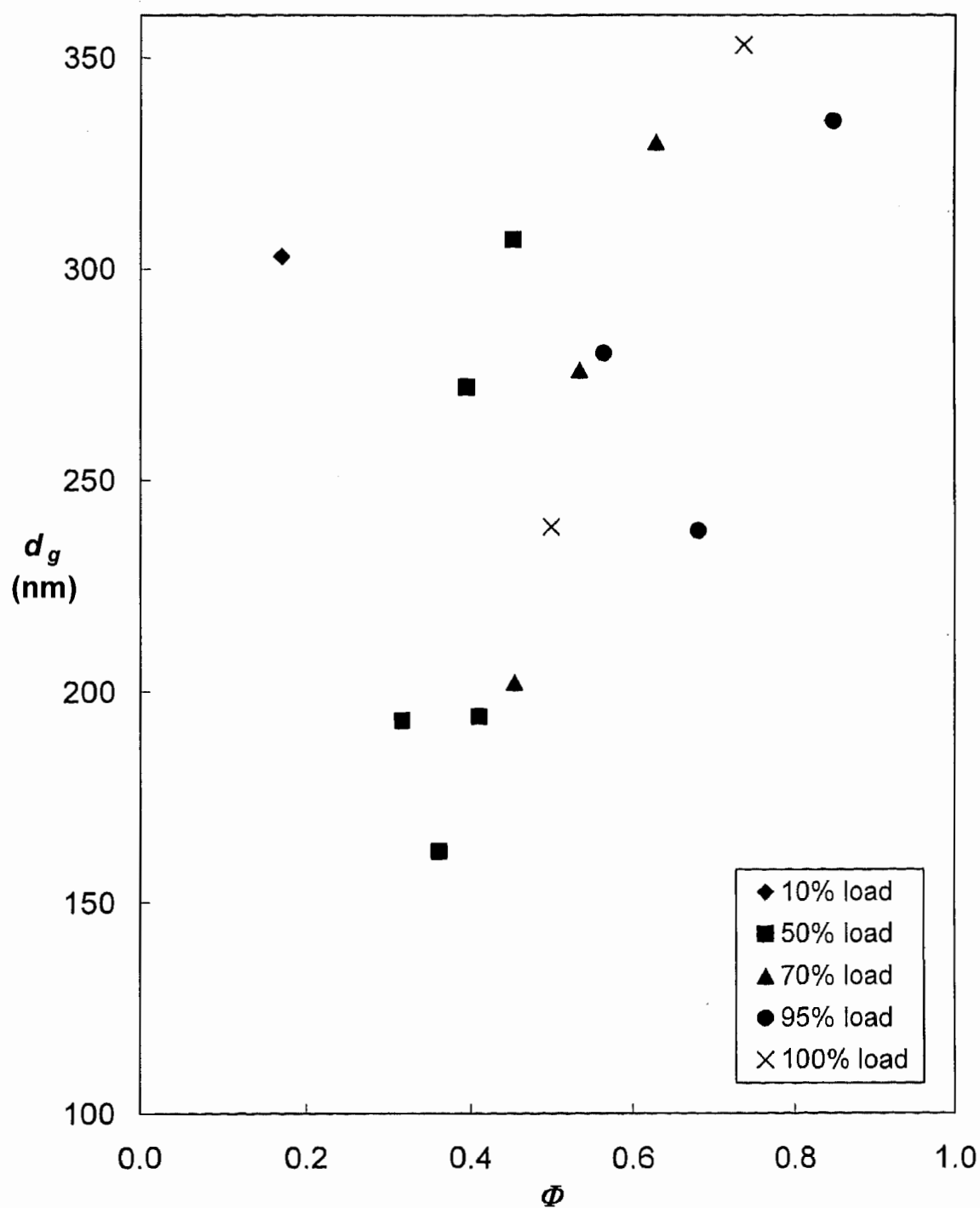


Figure 4.16. Aggregate gyration diameter as a function of overall equivalence ratio

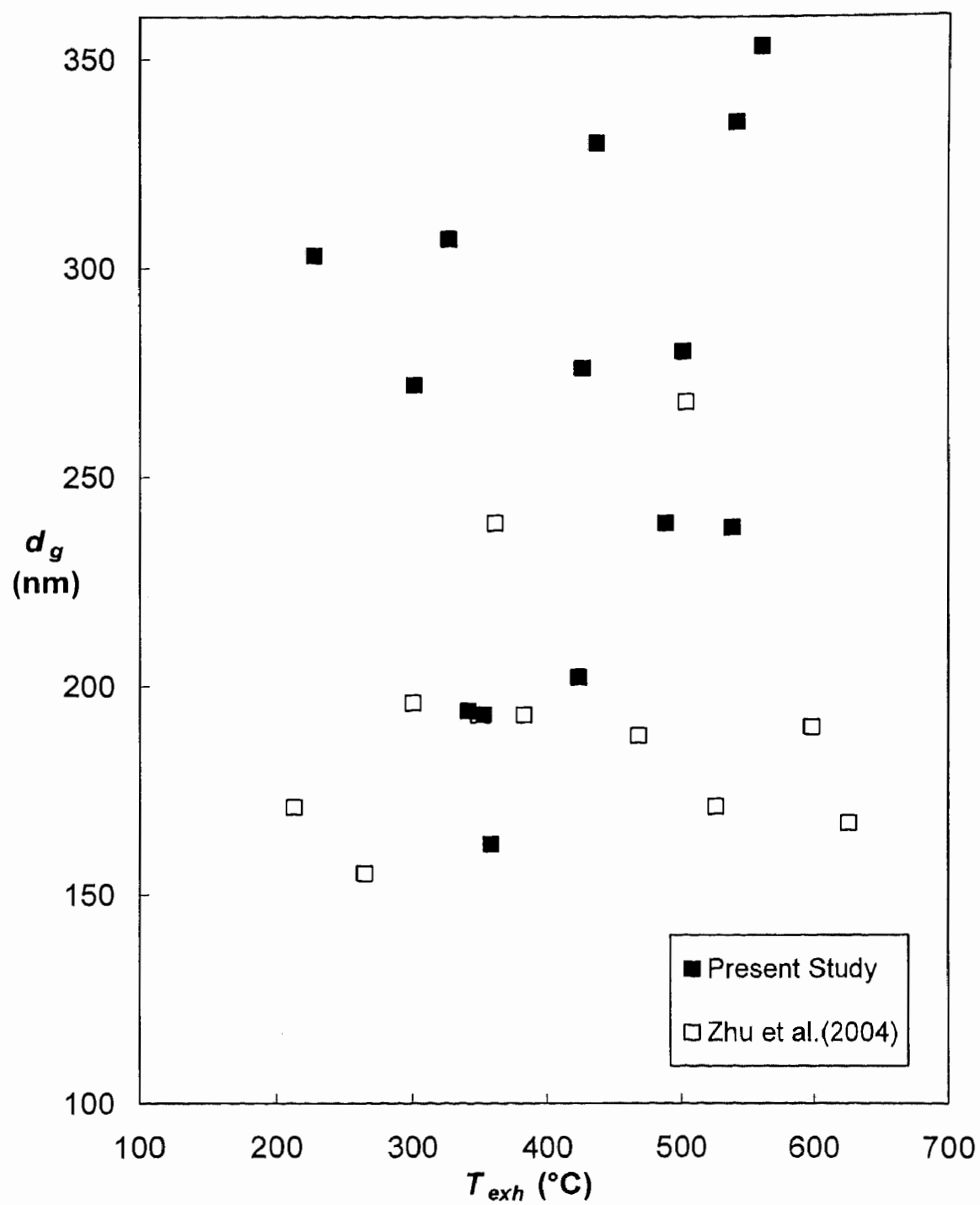


Figure 4.17. Aggregate gyration diameter as a function of exhaust temperature

generally composed of a larger number of primary particles than those at lower temperatures, which would also contribute to the increase in size. This is due to the increase in fuel supplied to diesel engine at higher loads.

The dependence of aggregate size on engine speed was also considered. The trend for aggregate gyration diameter as function of engine speed is displayed in Figure 4.18. For the individual loads, aggregate gyration diameters appeared to decrease with engine speed, similar to the trend observed by Zhu et al., (2004).

A discussion of aggregate sizes cannot neglect to account for mobility measurements. Park et al., (2004) recently reported that mobility diameter is nearly equivalent to an aggregates area equivalent diameter. Based upon this observation area equivalent diameters were calculated for the set of engine conditions studied. Similar to diameter of gyration, the area equivalent diameter, d_a , increased with increasing engine load as seen in Figure 4.19. A study by Virtanen et al., (2004) measured diesel particulates using a scanning mobility particle sizers (SMPS). Number distributions measured from a passenger car were in the size range of 70 to 100 nm, with volume distributions ranging from 200 to 400 nm as the engine load was increased from normal road loading to a 50% loading condition. Kelly et al., (2003) performed a similar study using a SMPS, reporting that the mobility diameter increased from 48 to 88 nm for a new diesel engine as load was increased from 80 to 90 percent and that for an older model diesel engine the mobility diameter increased from 46 to 96 nm for an increase in load from 2 to 23 percent. In general the mobility diameters reported by these two studies are smaller than the equivalent area diameters of the present study; but, the trends with respect to engine load are in agreement for the limited range of conditions.

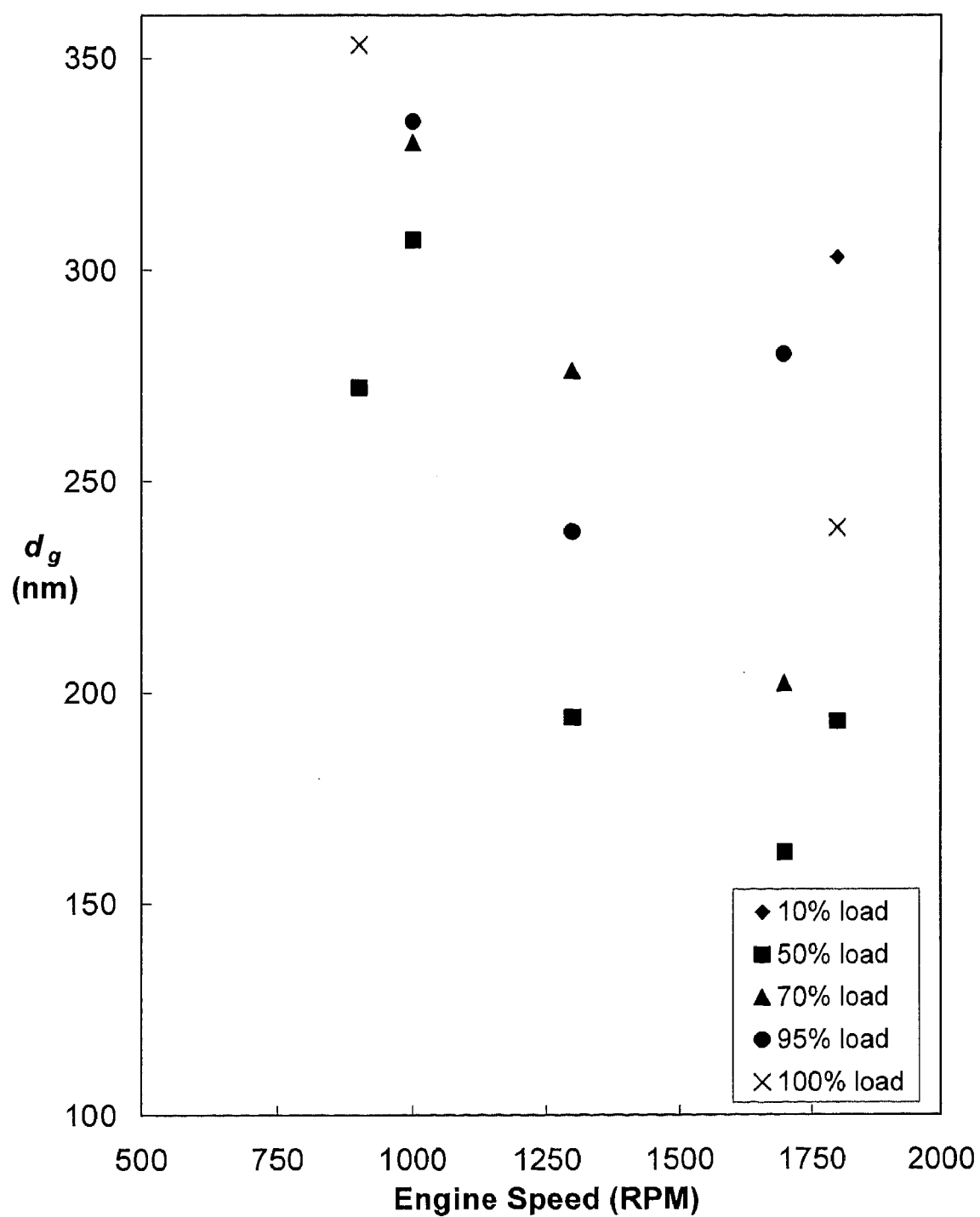


Figure 4.18. Aggregate gyration diameter as a function of engine speed

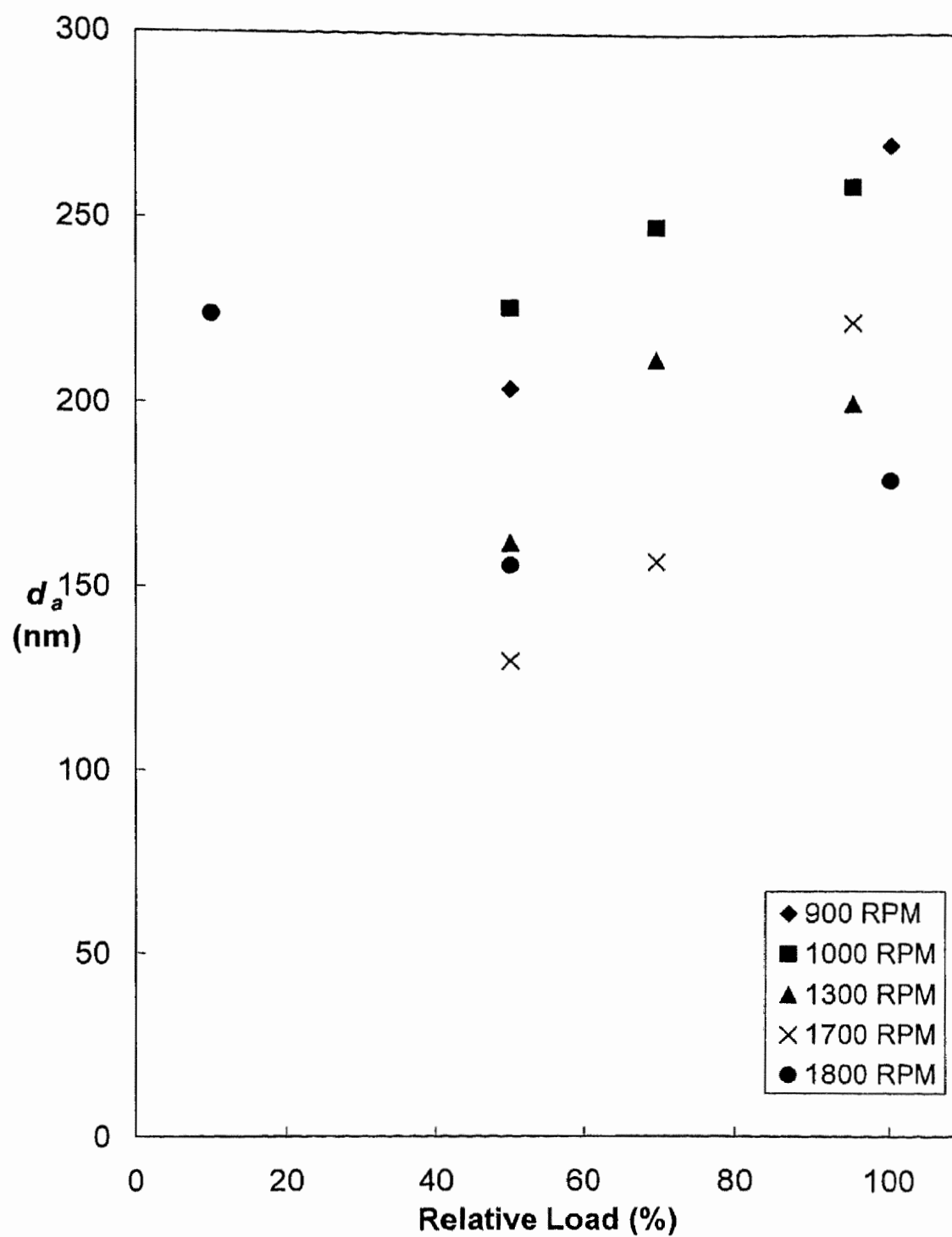


Figure 4.19. Area equivalent diameter as a function of engine load

4.6. SOOT VOLUME FRACTIONS

Estimations of soot volume fractions, f_v , from the engine were calculated based upon techniques used and developed by Koylu et al., (1997). The thermophoretic mass flux of particles to the collection surface was estimated by:

$$j_w'' \cong D_T \frac{Nu_x}{2x} \left[1 - \left(\frac{T_w}{T_g} \right)^2 \right] \rho_p f_v \quad (7)$$

where D_T is the thermophoretic diffusivity, T_w and T_g are the collection surface temperature and gas temperatures respectively, Nu_x is the local Nusselt number, and ρ_p is the soot density estimated as 1.8 kg/m^3 . Additionally the mass flux of particles deposited on the collection surface is :

$$\dot{m}'' = \frac{\rho_p V_p}{A_i t_s} \quad (8)$$

By assuming that the majority of mass is deposited by thermophoresis and constant wall temperature, these two fluxes can be equated $j_w'' \approx \dot{m}''$. Then, the soot volume fraction can be represented by

$$f_v = \xi \frac{V_p}{A_i t_s} \quad (9)$$

$$\xi = \frac{2}{D_T} \frac{x}{Nu_x} \left[1 - \left(\frac{T_w}{T_g} \right)^2 \right]^{-1} \quad (10)$$

The volume of particles deposited on the grid surface, V_p can be measured by knowing the spherule diameter and the number of spherules for each aggregate for each condition:

$$V_p = \frac{\pi d_p^3}{6} \sum_i N_i \quad (11)$$

Substituting equations 11 and 10 into equation 9, and using the expressions for thermophoretic diffusivity and local Nusselt number from Hu et al. (2003), the following expression for soot volume fraction is obtained:

$$f_v = 58454 \left(\frac{x}{u_g} \right)^{0.5} (T_g)^{-1.65} \left[\frac{T_w + T_g}{2} \right]^{0.825} \left[1 - \left(\frac{T_w}{T_g} \right)^2 \right]^{-1} (A_i t_s)^{-1} d_p^3 \sum_i N_i \quad (12)$$

where u_g is the gas velocity and A_i is the total image area for each condition. In the calculation of soot volume fractions, the collection surface temperature was assumed to be roughly that of the ambient, approximated by using a value of 300 K. Gas temperatures were measured downstream from the sampling location via a thermocouple in the exhaust pipe. Sampling times, t_s , were determined from calibration of the sampling equipment. The length x was presumed to be 1.525 mm, corresponding to the middle of the microscope grid. Exhaust gas velocity was estimated by conservation of mass from

the engine and assuming an area averaged velocity. With known mass flow rates for fuel and air, the mass flow rate exiting the engine was estimated by summing the fuel and air rates. By assuming a density to roughly that of air at a given exhaust temperature and assuming the exhaust pipe diameter at four inches, an estimate for u_g could be calculated. Based on this technique, soot volume fractions ranged from $2(10^{-3})$ to $2(10^{-1})$ ppm, increasing with equivalence ratio as shown in Figure 4.20. These estimates for soot volume fraction are the first to be reported implementing thermophoretic sampling techniques in a diesel engine.

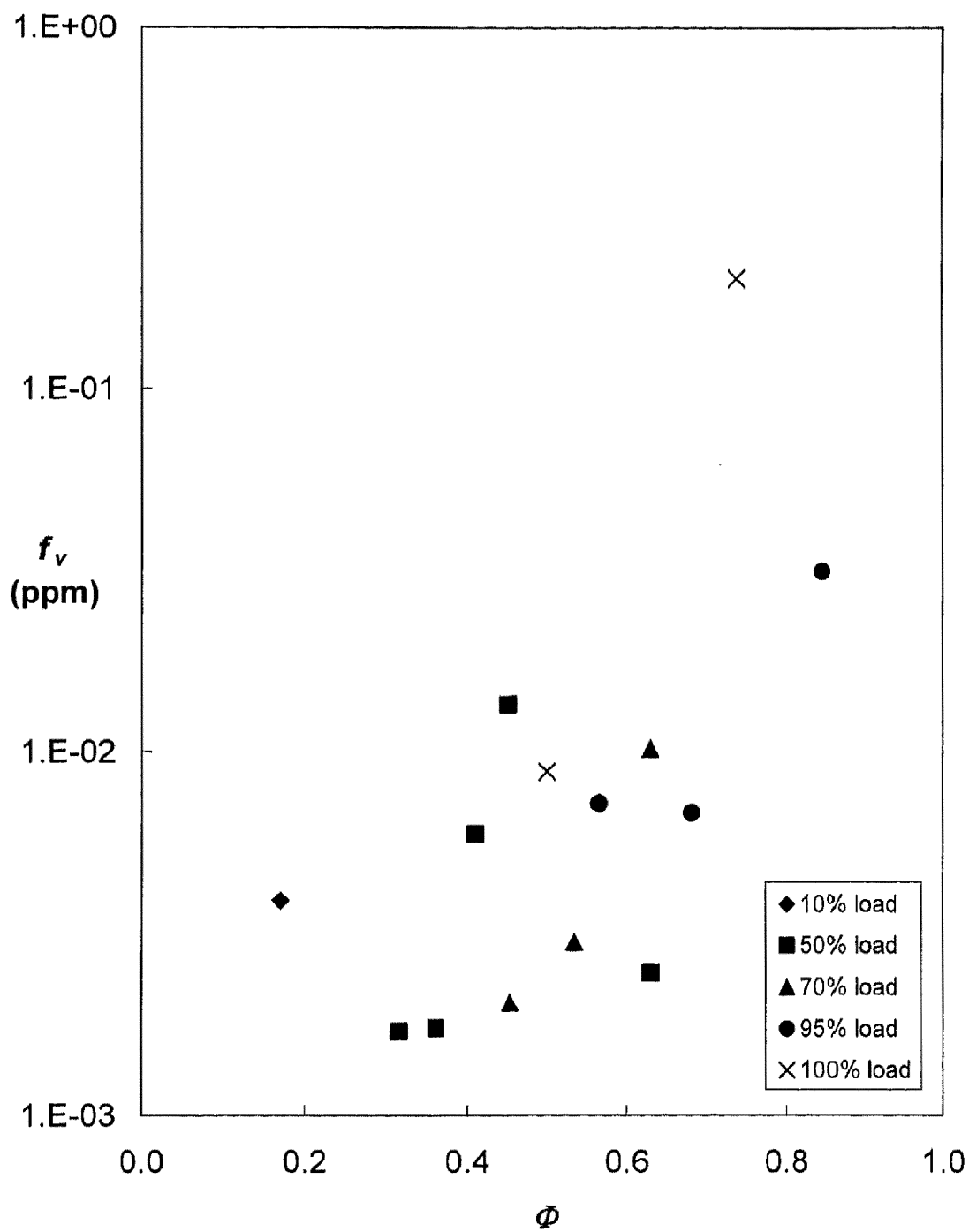


Figure 4.20. Soot volume fraction as a function of equivalence ratio

5. DISCUSSION

5.1. SPHERULE DIAMETERS

Mean spherule diameters tended to increase with engine load, exhaust temperature and overall equivalence ratio. Each of these variables is related and should be discussed jointly. Diesel engines operate under fuel lean conditions with soot being produced in the locally fuel-rich mixtures ($\Phi=1.0-1.2$) within the cylinder (Heywood, 1988). These locally fuel-rich regions are where the formation of soot particles occurs. Due to the complexities of diesel combustion, an examination of soot formation and oxidation within laboratory flames is beneficial to understanding these trends.

After individual spherules are initially formed, growth is sustained by coagulation and by chemical interaction. Increase in spherule size by coagulation is by pre-existing particles combining to form larger particles. The increase in diameter from chemical interaction is controlled by the addition of gas phase material onto the particle surface. These growth mechanisms are still researched in laboratory flames and cannot be directly related to the trends observed in diesel engines. However, the spherules size depends on oxidation as well as surface growth.

In the experiments performed by Santoro and Miller (1987), particle oxidation was decreased by increasing fuel flow rates in a laminar diffusion flame, similar to increasing engine load. Flower et al. included in their discussion of high pressure flames that soot oxidation may be inhibited by a decrease in temperature due to radiative losses from high soot concentrations, similar to the high pressure environment with the engine cylinder. These trends are summarized by Kittelson's (1998) statements that higher

values of Φ will lead to increased rate of formation of carbon and a decreased rate of oxidation, supporting the trends observed for the present study.

Spherule diameter also showed dependence on engine speed decreasing with increased engine speed. Engine speed is related to the characteristic time available for soot formation. Due to the rapid formation rates (~ 5 ms) of spherules it is unlikely that residence time could solely contribute to the variation of spherule size. A wider range of conditions needs to be considered in order to accurately determine the role of engine speed on spherule size.

5.2. AGGREGATE SIZES

The majority of particles emitted from the engine would not contribute much to the particulate mass being produced, but represent the greatest risk to health, due to their sizes of less than $1\text{ }\mu\text{m}$. Currently, particulate matter regulations are mass based with regulations on a $2.5\text{ }\mu\text{m}$ size. The measurements from the present study suggest that current sizing standards may be inadequate.

The increase in aggregate gyration diameter for load, equivalence ratio and exhaust temperature is related to the discussion of the trends observed for spherule diameters. Increasing load by the addition of fuel will increase the amount of carbon formation, leading to larger aggregates composed of many particles, in agreement with the observations made by Kittelson (1998).

Engine speed was also a factor in determining overall aggregate size. As engine speed increased, the aggregate gyration of diameter decreased. After the formation of spherules during the combustion process, spherules begin to aggregate. The process of

aggregation occurs on longer time scales than that of surface growth for spherules. Therefore, aggregate sizes would be more susceptible to the effect of the reduction in residence time by increasing engine speed. This would limit the time allowed for aggregation forcing smaller aggregates to be emitted from the engine as a result.

6. CONCLUSIONS AND RECOMMENDATIONS

6.1. CONCLUSIONS

Soot particles were collected from the exhaust gases of a John Deere 6059T diesel engine by thermophoretic sampling for various loads and speeds. Samples were photographed using TEM and analyzed with digital imaging software. A summary of all measurements can be found at the end of this section in Table 6.1.

Soot aggregates are composed of spherical primary particles and have fractal-like geometries. Graphitic nanostructure was not observed as has been reported in the literature. The engine produced individual spherules in greater amounts at increased loads. Primary particles followed a normal size distribution and were in the range of 20 to 35 nm in diameter. The particles increased in diameter with engine load, overall equivalence ratio and exhaust temperature. Particle diameter appeared to decrease for the range of speeds considered.

Aggregates measured from this engine had mean diameters of gyration from 160 to 350 nm with increasing sizes as a function of exhaust temperature, overall equivalence ratio and engine load. Similar to spherules, aggregate diameters appeared to decrease with increased engine speed. Almost all the aggregates were below 1 μm .

Fractal properties for the soot were characterized at different loading conditions by an average fractal dimension and fractal pre-factor of 1.77 ± 0.14 and 1.8 ± 0.5 respectively. Due to the narrow range of fractal dimensions it was concluded that aggregate morphology was independent of engine condition and that diesel soot can be represented by universal fractal properties.

Estimates for soot volume fractions were obtained using techniques developed from thermophoretic sampling, with values ranging from 0.002 to 0.2 ppm, increasing with overall engine equivalence ratio. This is the first study that this technique was used to measure soot volume fraction in a diesel engine.

The physical properties of diesel soot were similar to those measured from laboratory flames. This merits the continued study of these flames, as they can provide models for soot processes in more complicated combustion environments. These observations can lead to better development of emission controls and assist in legislative guidelines for allowable soot sizes.

Table 6.1. Summary of particulate measurements

Relative Load %	Speed RPM	d_p Nm	d_g nm	d_a nm	D_f	k_f	f_v ppm
10	900	29.2	N/A	N/A	N/A	N/A	
50	900	25.7	272	204	1.84	1.43	1.3E-02
100	900	29.2	353	270	1.92	1.29	2.0E-01
50	1000	33.2	307	226	1.65	2.03	5.9E-03
70	1000	27.9	330	248	1.76	1.87	1.0E-02
95	1000	35.1	335	259	1.76	1.86	3.1E-02
50	1300	19.7	194	162	1.72	2.37	1.7E-03
70	1300	29.7	276	212	1.88	1.31	3.0E-03
95	1300	28.9	238	200	1.82	1.82	6.8E-03
50	1700	23.9	162	130	1.87	1.4	1.7E-03
70	1700	28.5	202	157	1.75	1.62	2.0E-03
95	1700	26.9	280	222	1.73	2.18	7.2E-03
10	1800	24.5	303	224	1.68	2.26	3.9E-03
50	1800	20.5	193	156	1.74	2.09	2.5E-03
100	1800	23.4	239	179	1.71	1.94	8.8E-03

6.2. RECOMMENDATIONS

Engine operating conditions are typically characterized by the speed and load during operation. Some variables not considered during this study that are linked to diesel operation are: fuel injection timing, the amount of in-cylinder turbulence and the amount of recirculated exhaust gas (EGR) used. Various studies have been completed studying the effects these variables have on soot formation and destruction. Measurements by thermophoretic sampling have yet to be made. Accurately determining the effects of these operating parameters would provide scientists and engineers additional knowledge to reduce diesel particle emissions. Furthermore, the differences between the particulate emissions from different types of internal combustion engines (diesel and gasoline) should be investigated.

APPENDIX

EXPERIMENTAL UNCERTAINTIES

Experimental uncertainties and estimates were calculated using methods identical to Hu et al., (2003). In this analysis uncertainties of measured quantities, $w(R)$ for any $R(x_1, x_2, \dots, x_n)$, subject to n independent parameters is calculated by the root sum square method:

$$w(R) = \left[\sum_i^n \left(w(x_i) \frac{\partial R}{\partial x_i} \right)^2 \right]^{1/2} \quad (\text{A.1})$$

where $w(x_i)$ is estimated uncertainty of the individual x_i 's. From equation A.1 the confidence level for $w(R)$ and $w(x_i)$ will be the same. All uncertainties for the present study are based on the 95% confidence level.

Estimates for spherule diameter and maximum aggregate length are 5% error and aggregate areas in 10% error. Additional uncertainties were calculated following the previously developed methods:

$$w(A_p) = \frac{1}{2} \pi d_p w(d_p) \quad (\text{A.2})$$

$$w(N) = \sqrt{\left[-1.09 A_a^{1.09} A_p^{-2.09} w(A_p) \right]^2 + \left[1.09 A_a^{0.09} A_p^{-1.09} w(A_a) \right]^2} \quad (\text{A.3})$$

The fractal dimension and the fractal prefactor are obtained by evaluating the slope and the intercept of the $\ln(N)$ vs. $\ln(L/d_p)$ line. For M analyzed aggregates, uncertainties for D_f and k_L are estimated in the following equations:

$$w(D_f) = \sqrt{\sum_{i=1}^M \left(\frac{\partial D_f}{\partial \ln(N_i)} \right)^2 w[\ln(N_i)]^2 + \sum_{i=1}^M \left(\frac{\partial D_f}{\partial \ln\left(\frac{L}{d_p}\right)_i} \right)^2 w\left[\ln\left(\frac{L}{d_p}\right)_i\right]^2} \quad (\text{A.4})$$

$$w(k_L) = k_L \sqrt{\sum_{i=1}^M \left(\frac{\partial \ln(k_L)}{\partial \ln(N_i)} \right)^2 w[\ln(N_i)]^2 + \sum_{i=1}^M \left(\frac{\partial \ln(k_L)}{\partial \ln\left(\frac{L}{d_p}\right)_i} \right)^2 w\left[\ln\left(\frac{L}{d_p}\right)_i\right]^2} \quad (\text{A.5})$$

where

$$w[\ln(N)] = \frac{w(N)}{N} \quad (\text{A.7})$$

$$w\left[\ln\left(\frac{L}{d_p}\right)\right] = \sqrt{\left(\frac{w(L)}{L}\right)^2 + \left(\frac{w(d_p)}{d_p}\right)^2} \quad (\text{A.8})$$

Table A.1. estimated experimental uncertainties

Speed	Load	$w(d_p)$	$w(d_g)$	$w(D_p)$	$w(k_p)$
(RPM)	(%)	\pm (nm)	\pm (nm)	\pm	\pm
900	10	2	N/A	N/A	N/A
900	50	2	33	0.05	0.33
900	100	2	49	0.02	0.22
1000	50	2	39	0.09	0.41
1000	70	2	44	0.08	0.36
1000	95	2	43	0.09	0.35
1300	50	2	24	0.12	0.66
1300	70	2	37	0.10	0.31
1300	95	1	39	0.09	0.32
1700	50	1	38	0.12	0.27
1700	70	2	32	0.13	0.41
1700	95	3	50	0.13	0.63
1800	10	1	49	0.10	0.55
1800	50	1	23	0.10	0.45
1800	100	1	30	0.09	0.45

BIBLIOGRAPHY

- Braun, A., Shah, N., Huggins, F.E., Huffman, G.P., Wirick, S., Jacobsen, C., Kelly, D., Sarofim, A.F., "A study of diesel PM with X-ray microspectroscopy." *Fuel*, 83 (2004): 997-1000.
- Dobbins, R.A., and Megaridis, C.M., "Morphology of flame-generated soot as determined by thermophoretic sampling." *Langmuir*, 3 (1987): 254-259.
- Eisner, A.D., and Rosner, D.E., "Experimental studies of soot particle thermophoresis in nonisothermal combustion gases using thermocouple response techniques." *Combustion and Flame*, 61 (1985): 153-166.
- Flower, W.L., "An investigation of soot formation in axisymmetric turbulent diffusion flames at elevated pressure." *Twenty-Second Symposium (International) on Combustion/The Combustion Institute*, (1988): 425-435.
- Harris, S.J., Maricq, M.M., "Signature size distributions for diesel and gasoline engine exhaust particulate matter." *Journal of Aerosol Science*, 32 (2001): 749-764.
- Heywood, J. Internal Combustion Engine Fundamentals. New York: McGraw-Hill, 1988.
- Hu, B., Yang, B., Koylu, U.O., "Soot measurements at the axis of an ethylene/air non-premixed turbulent jet flame." *Combustion and Flame*, 134 (2003): 93-106.
- Kennedy, I.M., "Models of soot formation and oxidation." *Prog. Energy Combust. Sci.*, 23 (1997): 95-132.
- Kerry, K.E., Wagner, D.A., Lighty, J.S., Sarofim, A.F., Rogers, C.F., Sagebiel, J., Zielinska, B., Arnott, W.P., Palmer, G., "Characterization of exhaust particles from military vehicles fueled with diesel, gasoline, and JP-8." *Journal of the Air and Waste Management Association*, 53 (2003): 273-282.
- Kittelson, D.B., "Engines and Nanoparticles: A Review." *Journal of Aerosol Science*, 29 (1998): 575-588.
- Koylu, U.O., Faeth, G.M., "Structure of overfire soot in buoyant turbulent diffusion flames at long residence times." *Combustion and Flame*, 89 (1992): 140-156.
- Koylu, U.O., Xing, Y., Rosner, D.E. "Fractal morphology analysis of combustion generated-aggregates using angular light scattering and electron microscope images." *Langmuir*, 11 (1995): 4848-4854.

- Koylu, U.O., McEnally, C.S., Rosner, D.E., Pfefferle, L.D., "Simultaneous measurements of soot volume fraction and particle size/microstructure in flames using a thermophoretic sampling technique." *Combustion and Flame*, 110 (1997): 494-507.
- Lee, K.O., Cole, R., Sekar, R., Choi, M.Y., Kang, J.S., Bae, C.S., Shin, H.D., "Morphological investigation of the microstructure, dimensions, and fractal geometry of diesel particulates." *Proceedings of the Combustion Institute*, 29 (2002): 647-653.
- Neeft, J.P.A., Makkee, M., Moulijn, J.A., "Diesel particulate emission control." *Fuel Processing Technology*, 47 (1996): 1-69.
- Park, K., Kittelson, D.B., McMurry, P.H. "Structural properties of diesel exhaust particles measured by transmission electron microscopy (TEM): Relationships to particle mass and mobility." *Aerosol Science and Technology*, 38 (2004): 881-889.
- Santoro, R.J., Miller, J.H., "Soot particle formation in laminar diffusion flames." *Langmuir*, 3 (1987): 244-254.
- Skillas, G., Kunzel, S., Burtscher, H., Baltensperger, U., Siegmann, K., "High fractal-like dimension of diesel soot agglomerates." *Journal of Aerosol Science*, 29 (1998): 411-419.
- Shi, J.P., Mark, D., Harrison, R.M., "Characterization of particles from a current technology heavy-duty diesel engine." *Environmental Science and Technology*, 34 (2000): 748-755.
- Van Gulijk, C., Marijnissen, J.C.M., Makee, M., Moulijn, J.A., Schmidt-Ott, A., "Measuring diesel soot with a scanning mobility particle sizer and an electrical low-pressure impactor: performance assessment with a model for fractal-like agglomerates." *Journal of Aerosol Science*, 35 (2004): 633-655.
- Virtanen, A.K.K., Ristimäki, J.M., Vaaraslahti, K.M., Keskinen, J., "Effect of engine load on diesel soot particles." *Environmental Science and Technology*, 38 (2004): 2551-2556.
- Warheit, D., "Nanoparticles: health impacts?," *Materials Today*, (2) (2004):32-35.
- Wentzel, M., Gorzawski, K., Naumann, H., Saathoff, H. Weinbruch, S., "Transmission electron microscopical and aerosol dynamical characterization of soot aerosols." *Journal of Aerosol Science*, 34 (2003): 1347-1370.
- Zhu, J., Lee, K.O., Yozgatligil, A., Choi, M.Y. "Effects of engine operating conditions on morphology, microstructure, and fractal geometry of light-duty diesel engine particulates." *The Proceedings of the Combustion Institute*, 30 (2005): 2781-2789.

VITA

Adam Neer was born January, 12, 1980 in Independence, Missouri. He completed his elementary and high school education in Joplin, Missouri. He then briefly attended Missouri Southern State University and transferred to the University of Missouri-Rolla, where he obtained his Bachelor of Science degree in Mechanical Engineering in 2003.

He began his graduate studies at the University of Missouri-Rolla starting during August 2004. During this time, he worked under the supervision of Dr. Umit Koylu conducting research on diesel engine emissions. In October of 2004 he attended the annual conference of the American Association for Aerosol Research (AAAR) held in Atlanta, Georgia, and presented his work. His work was also presented at the 4th Joint meeting of the U.S. sections of the Combustion Institute during March of 2004 in Philadelphia, Pennsylvania. A journal paper detailing his work is in preparation for submittal to Combustion and Flame. He received his Master of Science degree in Mechanical Engineering in August 2005.